95-177

NATIONAL WATER RESEARCH INSTITUTE

INSTITUT NATIONAL de RECHERCHE sur les EAUX

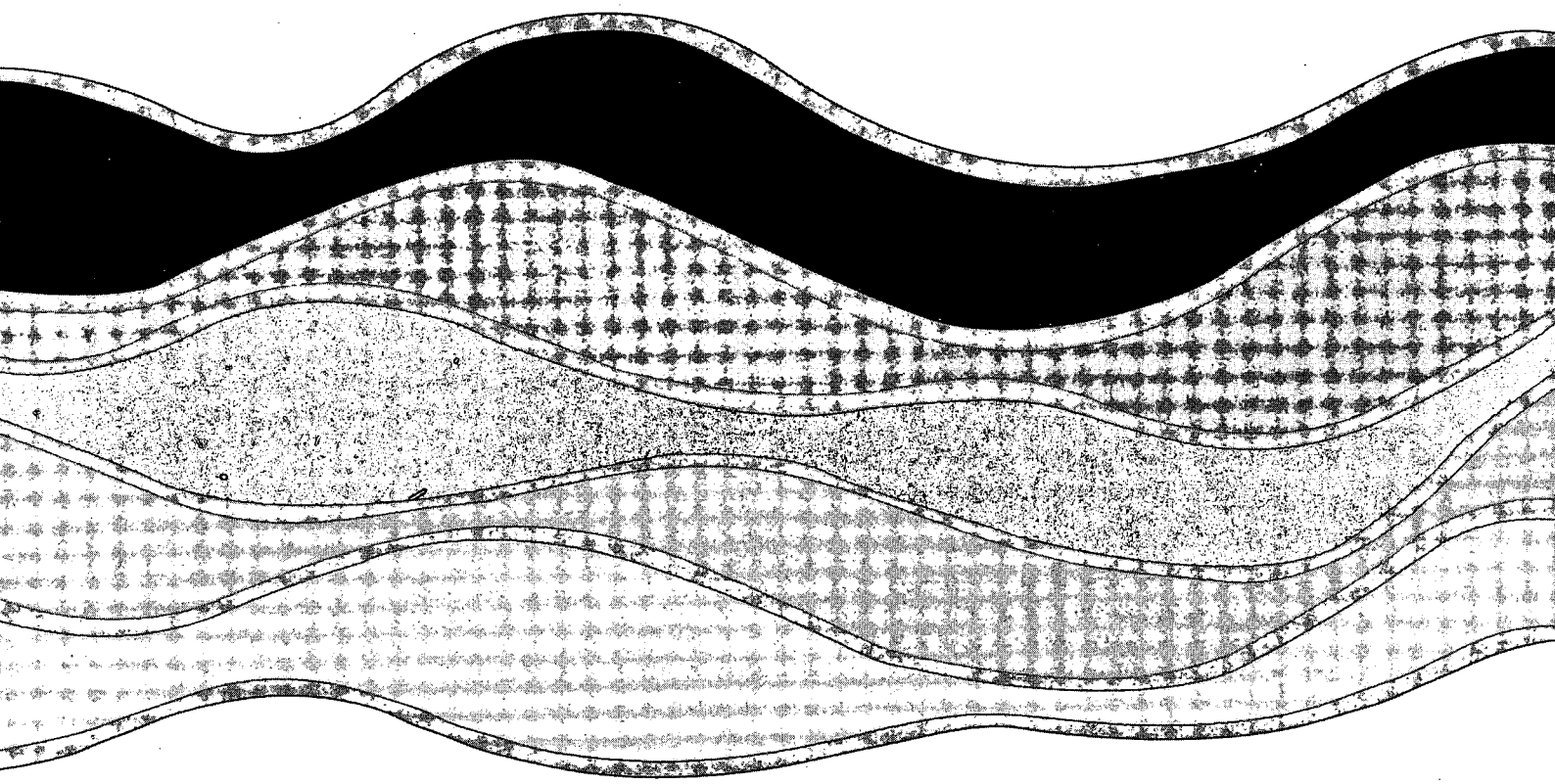

MODELLING THE FATE OF CONTAMINANTS IN LARGE RIVER PLUMES

J.A. Stronach, C.R. Murthy and T.S. Murty

NWRI Contribution No. 95-177

MODELLING THE FATE OF CONTAMINANTS IN LARGE RIVER PLUMES

J.A. Stronach
Seaconsult Marine Research Ltd.
8805 Osler Street
Vancouver, B.C. V6P 4G1

C.R. Murthy
National Water Research Institute
Canada Centre for Inland Waters
867 Lakeshore Road, P.O. Box 5050
Burlington, Ontario L7R 4A6

T.S. Murty
Institute of Ocean Sciences
Department of Fisheries and Oceans
P.O. Box 6000
Sidney, B.C. V8L 4B2

July, 1994

MANAGEMENT PERSPECTIVE:

The fate of pollutants, nutrients as well as contaminants, discharged by large rivers into the coastal waters is an important environmental issue. The residence time and the degree of accumulation of contaminants in the sediments are determined partly by physical exchange processes and partly by biotic processes active in the nearshore/offshore regions. The Niagara river plume in Lake Ontario and the Fraser river plume in the Strait of Georgia are of similar dimensions, and arise from rivers with discharges of comparable magnitude. Considering these two river plume systems, a number of important differences are immediately obvious. The Strait of Georgia has strong tides and its waters are saline. On the other hand Lake Ontario has no tides and its water is fresh. A third difference is that, although both water bodies have approximately the same dimensions, the Strait of Georgia is topographically more complex. Each of these differences has consequences on the hydrodynamics of the system, and the type of modelling required to successfully calculate velocity distributions for a pollutant transport model. Both rivers receive significant land derived sediment loads. Since fine sediments play strong role in the pathways and fate of toxic contaminants, modelling of these pathways is strongly controlled by the suspended sediment regime. Two different modelling scenarios are presented to simulate the mixing of the river plume in the coastal zone and to determine the horizontal distribution of contaminants in water and sediments within the river plume. The results provides a basis to develop management strategies to control the discharge of toxic contaminants into the coastal waters.

ABSTRACT

The Niagara River plume in Lake Ontario and the Fraser River plume in the Strait of Georgia are of similar spatial dimensions, and arise from rivers with discharges of similar magnitude. Both rivers receive significant loads of toxic wastes. The contaminant fate aspects of a previously-developed model for the Niagara River plume (Stepien *et al.*, 1987) have been applied to contaminant modelling in the Fraser River plume in the Strait of Georgia, and are described in this report, along with a review of the Niagara River plume modelling. Since fine sediments play a strong role in the pathways and fate of toxic contaminants, modelling of contaminant pathways also requires a quantitative description of the suspended sediment regime. Two different modelling scenarios will be described. For the Niagara River plume, a near field model has been developed. The hydrodynamics are barotropic, since the water column is well-mixed due to the presence of the Niagara River sand bar. For the Fraser River plume, a far field model has been developed. The hydrodynamics are baroclinic, since a strong pycnocline separates the plume from the underlying water. The flow fields produced by these models are used to derive a generalized transport/diffusion model to simulate the horizontal distributions of contaminants. The model partitions the contaminant between the dissolved and the adsorbed phases. To simulate this partitioning, the contaminant transport module computes both suspended sediment concentration and total contaminant concentration. The partitioning between dissolved and adsorbed phases is determined by an equilibrium partition coefficient. Contaminant concentrations in the Niagara River plume simulations compared reasonably well with observations. For the Fraser River plume, observational data for contaminants is presently unavailable, but the modelled sediment distribution compares well with observations. In both cases, the suspended sediment load plays a significant role in contaminant transport and distribution.

1 INTRODUCTION

The fate of contaminants discharged by the Fraser River into the Strait of Georgia is an important issue in view of continued and increasing utilization of the Strait, as well a scientific uncertainties concerning the long-term fate of contaminants. Similar concerns apply to contaminants carried by the Niagara River into Lake Ontario. Numerical models describing the distribution of contaminants in these water bodies will greatly improve understanding of the potential impacts of continued contaminant disposal at present rates, and the recovery period as contaminant discharges become increasingly regulated and reduced. This paper describes a preliminary investigation into modelling the transport and fate of contaminants which are carried into the Strait of Georgia by the Fraser River. Comparison is also made with the Niagara River plume in Lake Ontario.

Considering these two river plume systems, a number of important differences are immediately obvious. The Strait of Georgia has strong tides and its waters are saline. On the other hand Lake Ontario has no tides and its water is fresh. A third difference is that, although both water bodies have roughly the same dimensions, the Strait of Georgia is topographically more complex. Each of these differences has consequences on the hydrodynamics of the system and the type of modelling required to successfully calculate velocities for a contaminant transport model. In addition, sediment loading is an order of magnitude larger in the Fraser River. Since fine sediments play a strong role in the pathways and fate of toxic contaminants, modelling of these pathways is also strongly controlled by the suspended sediment regime. Two different modelling scenarios will be described. For the Niagara River plume, a near field model has been developed. The hydrodynamics are barotropic, since the water column is well-mixed due to the presence of the Niagara River sand bar. For the Fraser River plume, a far field model has been developed. The hydrodynamics are baroclinic, since a strong pycnocline separates the plume from the underlying denser water. The flow fields produced by these models are used to drive a generalized contaminant transport model to simulate the horizontal distributions of contaminants. The model partitions the contaminant between the dissolved and the adsorbed phases. To simulate this partitioning, the contaminant transport module separately computes suspended sediment concentration and total contaminant concentration. The partitioning between the dissolved and adsorbed phases is controlled by an adjustable parameter, the partition coefficient, which is taken to be a constant for each of the simulations. Contaminant distributions computed for the Niagara River plume simulations compared reasonably well with observations. For the Fraser River plume, observational data for contaminants is presently unavailable, but the modelled sediment distribution compares well with observations. In both cases, the suspended sediment load had a significant effect on the contaminant transport distribution.

Circulation and contaminant transport modelling in the Niagara River plume have been discussed in Murthy *et al.* (1986); Lam (1978); Lam *et al.* (1984); Simons (1980); Murthy and Miners (1989); Stepien *et al.* (1987). Recent modelling activities have focussed on the near-field, such as the model described by Stepien *et al.*, (1987), which solves the contaminant transport equations in a region 40 km by 20 km, treating the Niagara River as a single point source.

The hydrodynamic component of the modelling for the Strait of Georgia is provided by the GF4 numerical model (Stronach *et al.*, 1988), which simulates the motion of the upper layer of water, incorporating the effects of tides, winds, river runoff and basin geometry. The advection and diffusion of contaminants is modelled in a similar manner to procedures for the Niagara River plume described in Stepien *et al.* (1987), in which the contaminant is partitioned between the dissolved phase and the phase adsorbed onto suspended sediment. The Strait of Georgia model discussed here considers two point sources, the South or Main Arm and the North Arm of the Fraser River, and covers the entire Strait of Georgia, extending 170 km to the north and 50 km to the south of the source region. This report is organized as follows. Sections 2 to 5 have parallel sub-sections, dealing with the Fraser Rive plume and the Niagara River plume individually. Section 2 describes the physical setting of the two plumes, and the state of knowledge of levels of contamination and contaminant fluxes. Section 3 describes observational programs which are relevant to this study. Section 4 describes the hydrodynamic and contaminant transport models for both systems, and section 5 describes their validation. Section 6 discusses some modelling scenarios in the Strait of Georgia. Section 7 summarizes the results, and reviews the steps which are necessary to better understand and model the fate of contaminants in the system.

2 THE PHYSICAL SETTING

Figure 1 is a map of the southern Strait of Georgia showing the Fraser River entering on the eastern side of the Strait. Figure 2 is a detailed map of the Fraser Estuary and the greater Vancouver region, showing the complex distributary system by which the Fraser River flows into the central part of the Strait of Georgia along its eastern shore. As shown in Figure 2, the Fraser River has three principal distributary mouths, the South Arm carrying about 85% of the total discharge, the North Arm carrying 10%, and the Middle Arm carrying about 5% (Anon., 1981). Each of these distributaries discharges through channels cut into wide intertidal flats, Roberts Bank to the south and Sturgeon Bank to the north.

For the purposes of the numerical modelling to be described in subsequent sections, the mouth of the South Arm is assumed to be located at the Sand Heads Lighthouse, situated at the end of a major training jetty extending 6 km from the town of Steveston. This jetty constrains the South Arm on the north side to a

well-defined navigation channel as it flows across the tidal flats. On the south side of the river, the shallow banks similarly constrain the bulk of the river flow to lie within the navigation channel, until the deep waters of the Strait of Georgia are encountered. Observed water motions on Roberts Bank (Crean *et al.*, 1988) are consistent with the assumption that the Main Arm is contained within its navigation channel.

Snow melt forms two thirds of the precipitation in the Fraser River drainage basin. Consequently, river flow peaks in late May or early June. Gauging stations maintained by Water Survey of Canada are situated at a number of locations along the river, the most relevant for this report being the gauge at Hope. Although there is some freshwater input into the Fraser River downstream of Hope, 90% of the river flow reaching the Strait of Georgia passes through the Hope section of the river. River discharge varies on average from a minimum of 600 $m^3 s^{-1}$ during the winter period to 8800 $m^3 s^{-1}$ during freshet. Flooding of the Fraser valley is occasionally a major problem, the most recent severe flood being in 1948, when discharge peaked at 15,200 $m^3 s^{-1}$. At the river mouth, the river water level is predominantly determined by tidal fluctuations in the Strait of Georgia. River velocities are similarly modulated by the tide, although there is a net residual flux to account for the net discharge of freshwater.

Tides in the Strait of Georgia are of the mixed type, with almost equal contributions from the diurnal and semi-diurnal constituents. The orientation of the Strait of Georgia is perpendicular to the river channel, so that tidal currents are directed across the river mouth. There is a significant amount of baroclinicity in tidal currents in the Strait of Georgia and one of the most significant baroclinic effect is the buoyant surface jet which results when the Fraser River enters the Strait: the Fraser River plume. This plume is characterized by a thin layer of brackish water of thickness 3 to 5 m in which currents are strongly dominated by the momentum flux from the constrained river flow, causing fresh water to move rapidly away from the river mouth, with maximum flow at about ¾ hour before low water.

In conjunction with this formation of a surface jet in the Strait, there is a complementary phenomenon in the river - the salt wedge (Hodgins, 1977; Ages, 1979; 1988). The salt wedge is a slug of salt water which typically moves upstream into the river on a rising tide, and is subsequently flushed out on a falling tide. The flow is more complex in detail: the wedge dynamics are dependent on the magnitude of the river discharge and on the tidal range on each cycle, so that the salt wedge may not necessarily be swept out on each ebb tide, depending on the tidal range. The river mouth also represents a transition region from horizontally one-dimensional flow to horizontally two-dimensional flow, accompanied by a large degree of vertical mixing. The fluxes of fresh water and salt water at the river mouth are thus quite complicated. For the model described here, a simplified approach will be taken, the freshwater flux being related to harmonic constants for the surface current at the river mouth.

Figure 3 shows Lake Ontario and an enlarged map of the Niagara River region, showing the 1-km grid used for the Niagara plume modelling discussed later in this paper. The river mouth geometry is considerably simpler than the Fraser River mouth, reflecting the lower sand load in sediments in the Niagara River and the different dynamics in the receiving basins.

The discharge magnitudes in the Niagara and Fraser river systems are similar, although the Niagara River daily discharge is reasonably uniform throughout the year, whereas the Fraser has a well defined freshet peak, with flow at freshet being typically ten times larger that mid-winter flows. The Niagara discharge is estimated at 7000 $m^3 s^{-1}$ (Murthy and Miners, 1989), compared to the Fraser River discharge which ranges from 600 $m^3 s^{-1}$ during mid-winter to 8800 $m^3 s^{-1}$ during a typical freshet. Because of modulation by the tide, the instantaneous Fraser River flow undergoes daily fluctuations which range from a near-zero upstream value at about high tide, to downstream flows exceeding twice the daily average value at about low tide. The Niagara River has a similar temporal variation, produced by flow variations which arise from the operating requirements of hydroelectric generation along the river, which result in a strong diurnal modulation of the daily discharge.

A major difference between the Fraser River and the Niagara River is the sediment load they carry. The annual Niagara River sediment load is approximately 4.7 million tons (Murthy and Miners, 1989). The annual Fraser River load varies between 12 and 30 million tons of sediment, 80% of which is carried during the freshet period between May 1 and July 15 (Milliman, 1980). Thus, the Fraser carries up to six times more sediment annually than does the Niagara, and most of the load is transported during a two and a half month period.

The geometry of the two river mouths is also different. In plan view, the Niagara has a single distributary channel terminated by a river mouth bar. This bar leads to locally increased currents, and to a vertically uniform distribution of density in the vicinity of the river mouth. The Fraser River, immediately upstream of its entrance to the Strait of Georgia, travels through a dredged channel, cut across a 5-km wide expanse of intertidal flats. It then discharges into deep water at the edge of the flats. The drop-off of the river bed at the edge of the flats is steep, and a river mouth bar does not form.

The receiving basins for the two rivers are also dissimilar. The Niagara plume discharges into Lake Ontario, a non-tidal inland lake in which the density contrast between the plume and the ambient water is due to thermal differences, and seldom exceeds 0.5 sigma-t units. The Fraser discharges into the Strait of Georgia, a tidal, salt water body, in which the density contrast between the plume and the ambient water is governed by salinity differences, which give rise to variations in density between the plume and the underlying water of up to 25 sigma-t units.

The level and nature of contaminants in the Niagara River are well documented, (Elder *et al.*, 1981; Warry and Chan, 1981; Allan *et al.*, 1983; Niagara River Toxics Committee, 1984). However, the corresponding information for the Fraser River is not as readily available, although sources of chlorophenolic compounds, for instance, are discussed in Carey and Hart, (1988). Similarly, the spatial distribution of contaminants in Lake Ontario is a subject of ongoing monitoring programs, and is discussed by Allan *et al.* (1983) and by Frank *et al.* (1979), among others. The spatial distribution of contaminants in the Strait of Georgia and the Fraser River Estuary is by contrast poorly known, although this distribution can possibly be inferred from maps of surficial sediments prepared by Pharo and Barnes (1976), particularly because of the important role that the settling of suspended sediment plays in the fate of contaminants.

3 OBSERVATIONAL PROGRAMS

The Fraser Plume

A number of observational programs have been carried out to describe the surface current pattern in the Strait of Georgia and in the Fraser River plume (Stronach, 1984; Thomas 1979; Giovando, 1972). These observations provide consistent descriptions of the plume based on drogue tracking experiments. Detailed salinity and temperature observations are not as readily available, mainly because the effort required to maintain drogue patterns did not allow an extensive network of CTD stations to be occupied during drogue tracking experiments. Nevertheless, sufficient data has been acquired to allow reasonable verification of model hydrodynamics (Stronach *et al.*, 1988). One of the major validation studies concerned a comparison of GF4-modelled salinities with surface bottle-cast data collected during conditions of both high and low river discharge, along a line from the river mouth to the northern limit of the Strait of Georgia, a distance of 180km. GF4 reproduced both the spatial gradients of salinity as well as the seasonal variation. The modelled currents tend to be somewhat smaller than observed using surface drogues, but the comparison is not entirely fair, as GF4 calculates an average current over the upper layer, whereas the drogues tended to occupy only the top half of the layer. Nevertheless, the comparison with the salinity distribution indicates that transport of scalars is calculated reliably, which is the most important criterion for contaminant transport modelling.

There are no data available on contaminant concentrations in the plume. Carey and Hart (1988) have examined contaminant concentrations in the Fraser River and found that the supply was sporadic for many chemicals, often triggered by a rainfall event.

The Niagara Plume

The contaminant modelling program for the Niagara River was coordinated with an intensive physical and chemical field program. In 1982, seawater samples on a grid throughout the plume were collected on seven cruise between April 13 and November 12. The principal outcome from these cruises was the selection of two compounds which could serve as tracers of the Niagara River Plume: 1,2,3,4-tetrachlorobenzene (1,2,3,4-TeCB), and 1,2,4-trichlorobenzene (1,2,4-TCB). Other compounds were either ubiquitous, or only present on a sporadic basis. In 1983, three cruises were involved. The water sampling procedure was modified to determine more accurately the partitioning of contaminant between dissolved and particulate components. In order to determine the velocity field during the 1983 cruises, up to 15 sail drogues per cruise were released about 1.5 km upstream of the river mouth, and tracked using a Mini-Ranger system until they had passed out of the area covered by the plume. The ship course pattern for seawater samples in these cruises was determined by observing the real-time drift pattern, in order to maximize the probability of sampling in the contaminant plume. The data for contaminant and sediment concentration and velocities allow a high degree of comparison between the Niagara River plume model and observations.

4 THE HYDRODYNAMIC AND CONTAMINANT TRANSPORT MODELS

The Niagara River Plume Hydrodynamic Model

The region around the mouth of the Niagara River has been found to be well mixed in the vertical, so that a barotropic model adequately describes the current field in that region. Thus, the two dimensional model described in Simons and Lam (1986) was used to provide the hydrodynamic component.

The Fraser River plume Hydrodynamic Model GF4

GF4 was developed in order to model the velocity field in the Fraser River plume, and hence is ideally suited to contaminant transport modelling (Stronach *et al.*, 1988). GF4 models the upper 1 to 5 m of the water column, and calculates velocities, salinity, and layer thickness on a 2-km grid. The variability in the upper layer thickness is governed by baroclinic processes in the model and can be related to the changing density profile as one proceeds away from the river mouth. The underlying water is assumed to be of uniform salinity, representing a seasonal average of intermediate and deep waters in the Strait of Georgia. Currents and pressure gradients in the lower layer are calculated by a vertically integrated tidal model, using the same 2-km grid as GF4.

The Strait of Georgia model was run from May 1 to June 15, 1988, using observed winds over that period, and historical values for the monthly mean

Fraser River discharge. All results in this report were taken from this 45-day period. This time period was chosen to coincide with sampling programs reported by Kostaschuk *et al.* (1989). Previous experience with GF4 indicated that the model comes to equilibrium in about 15 days from an initially uniform state. It has been assumed that a similar spin-up time is required for the contaminant and sediment models, and thus the modelled data after May 15 can be considered valid.

Contaminant Transport and Fate

The contaminant transport model was developed by adding two sub-models, one for suspended sediment and one for contaminants, to an existing hydrodynamic model. The two new sub-models incorporated both transport and diffusion of the relevant scalar field. The sediment model accounted for settling of sediment, and the contaminant model partitioned the contaminant into a fraction adhering to the sediment, and a dissolved fraction. Stepien *et al.* (1987) noted that the presence of suspended sediment had a significant effect on the concentration of contaminants, because contaminants have a tendency to be adsorbed onto sediment, and are then removed from the water column as the sediment sinks. The adsorbed amount is given by a partition coefficient relating the adsorbed concentration to the suspended sediment concentration:

$$C_P = \frac{\pi C_{SS}}{1 + \pi C_{SS}} C_T \qquad (1)$$

$$C_D = \frac{1}{1 + \pi C_{SS}} C_T \qquad (2)$$

where C_T, C_P and C_D are the total, particulate-adsorbed and dissolved concentrations, C_{SS} is the suspended sediment concentration and π is the partition coefficient. This partition coefficient was found to be reasonably constant in the Lake Ontario field study. The same value was used for the Strait of Georgia simulations, despite two significant differences between the systems:

1. The sediment levels are considerably higher in the Fraser River, and the difference in grain size distributions between the two systems is not parameterized;

2. The chemical regime in the Fraser River undergoes a profound change when the fresh water encounters salt water, giving rise to flocculation. This effect has not been incorporated in the simulations described here.

The transport and diffusion of the suspended sediment and total contaminant concentration were calculated according to equations (3) and (4) below, also taken from Stepien *et al.* (1987):

$$\frac{\partial hC_{ss}}{\partial t} + \nabla \cdot \bar{U}C_{ss} = K\nabla \cdot h\nabla C_{ss} - wC_{ss} \qquad (3)$$

$$\frac{\partial hC_r}{\partial t} + \nabla \cdot \bar{U}C_r = K\nabla \cdot h\nabla C_r - \frac{w\pi C_{ss}}{1 + \pi C_{ss}} C_T \qquad (4)$$

where $\bar{U}$ is the two-dimensional vertically integrated transport vector, h is the layer thickness for GF4 or the depth for the Niagara plume model, ∇ is the two dimensional spatial gradient operator, K is the horizontal eddy diffusion coefficient, and w is the net settling velocity.

Model Parameterizations

The horizontal eddy diffusion coefficient used for the Fraser River plume was 100 m^2/s for both sediment and contaminant, identical to the eddy viscosity. For the Niagara plume simulations, it was 0.1 m^2/s, based on dye diffusion studies (Murthy, 1969). These two numbers represent a large difference in the value of eddy diffusivity, and further modelling and observations in the Strait of Georgia will be required to determine if lower values of eddy diffusivity provide improved solutions.

In order to test the effect of sediment adsorption in the Fraser River plume, two simulations were done, one in which the partition coefficient was set at 0.077 L mg^{-1}, the average of the two values used by Stepien *et al.* (1987), and one in which it was set at 0.0 L mg^{-1}, to test the sensitivity of the contaminant distribution to the adsorption process.

Sediment Processes

For the Lake Ontario simulations, the sediment settling rate was determined by operating the model for three settling rates (1, 2, and 3 m/day), to determine the best fit to the observational data.

For the Strait of Georgia simulation, the sediment settling rate was determined from an independent set of field measurements. The sediment settling rate and the sediment concentrations at the river mouth were parameterized in terms of simple algebraic relations, discussed below. The net settling velocity w

is composed of two terms: the intrinsic settling velocity of suspended sediment in a stationary medium, as determined in laboratory measurements, and the downward turbulent flux, parameterized as a combination of entrainment and depletion velocities, calculated by GF4 and discussed in section 3.1. In the model described here, the two-way mixing process due to entrainment and depletion reduces to a one-way flux of contaminant, because contaminant concentrations in the underlying layer are assumed to be zero. Hence, of the two velocities calculated by GF4, only the depletion velocity is relevant to the sediment and contaminant models.

The intrinsic particle settling velocity required an ad hoc parameterization. In general, the sediment load is comprised of a range of grain sizes, and hence a range of settling velocities. Since a single constituent sediment model was used, the simulation of the intrinsic settling rate had to be approached in an empirical manner, which was developed as follows. Near the river mouth, the suspended sediment load contains a large fraction of sand which settles rapidly. At increasing distances from the river mouth, the grain size distribution shifts toward finer fractions, and the average settling speed is reduced. In order to simulate this shift in intrinsic settling speed with a single sediment fraction, the particle settling speed was made proportional to the square of the sediment concentration:

$$w = woC^2/C_o^2 \qquad (5)$$

where w_o was 1.0 cm s^{-1} and C_o was 1000 mg L^{-1}. As Equation (5) indicates, the settling velocity ranged quadratically from a maximum value 1 cm s^{-1} for a concentration of 1000 mg L^{-1} (the maximum river mouth concentration value), to values as small as 0.000025 cm s^{-1} for concentrations of 5 mg L^{-1}.

Hence, the settling speed is largest near the river mouth, and decreases with increasing distance from the river mouth. The river mouth concentration of sediment, the boundary condition for the sediment model, varies tidally, depending on the energy of the river flow. Initially, the relationship between concentration and instantaneous river flow was assumed to be linear. However, this parameterization did not produce sediment concentrations which compared favourably with observations. A reasonable calibration was achieved by making the river mouth concentration vary quadratically with river flow, as given by equation (6):

$$C = 500 \cdot (Q/9360)^2 \qquad (6)$$

A concentration of 500 mg L^{-1} was chosen to correspond to a flow of 9,360 m^3 s^{-1}, the average daily discharge for June. If the concentration give by equation (6) exceeded 1000 mg L^{-1}, it was reduced to 1000 mg L^{-1}.

The concentration of contaminant at the river mouth was not tidally modulated, but was set to a uniform value of 100 mg L^{-1}.

The instantaneous river discharge was determined by first interpolating a daily discharge value from the monthly mean daily discharge values, the latter assumed to apply on the 15th day of each month. The interpolated daily discharge was then tidally modulated, using harmonic constants for currents at the river mouth (Stronach, 1977).

Second-Order Numerical Advection

The Niagara plume model used finite difference methods as described in Simons and Lam (1986). In GF4, a second order, flux-corrected transport algorithm was used. The Arakawa C-grid used for GF4 naturally lends itself to the divergence form in which equations (3) and (4) are cast. The flux-corrected algorithm was implemented by first computing the updated contaminant or sediment field using a Lax-Wendroff estimate of the flux terms. These fluxes are then second order accurate in space. By itself this method generally produces an acceptable solution, but leads to small amplitude, small wavelength spatial oscillations and hence small negative values of the transported scalar at the leading and trailing edges of features such as the sediment plume.

The next step in the numerical process is to identify those cells in which the transport terms acting alone lead to either a negative value of concentration or a relative minimum in the concentration. For each of these cells, the unphysical scalar field was corrected by recalculating the transport terms using upstream differencing, a method which is first order accurate in space. The upstream differencing method suffers from considerable numerical dispersion which makes it unsuitable for the general transport process. However, its inherent numerical dispersion makes it suitable for correcting the spurious errors generated by the second order method on a cell by cell basis. Care was taken in implementing this algorithm that mass was conserved by recalculating the scalar field in all cells which were affected by the change in the order of the method for the flux calculation.

This flux-corrected method is considerably simpler than other implementations described for example by Zalesak (1979). It does not propagate a box-car shaped distribution through a grid as well as Zalesak's method, but it does propagate smoother distributions at least as well. Since the modelled contaminant distributions are relatively smooth and contain no mechanisms to generate steeper gradients, this scheme is well suited to contaminant modelling in natural water bodies.

5 MODEL CALIBRATION AND VERIFICATION

The verification of the GF4 hydrodynamic model has been discussed in Stronach *et al.* (1988). The limitations imposed by data availability did not allow extensive calibration and verification of the sediment and contaminant transport modules for the Strait of Georgia. It was possible, however, to calibrate in a limited manner the intrinsic settling velocity used in the sediment transport module. This was done by comparing the modelled distribution of suspended sediment along a line from Sand Heads to Porlier Pass with observations reported by Kostaschuk *et al.* (1989).

Figure 4a compares the observed and modelled results at a tidal phase corresponding to high river flow (14:00 PST, May 20), and Figure 4b compares them at a tidal phase corresponding to low river flow (7:00 PST, May 20, 1988). The agreement in Figure 4a is excellent, partly because the function specifying fall velocity was adjusted to agree with this curve. However, there are more measurement points than adjustable constants, so it is likely that the fall velocity function applies to other combinations of tide and river flow. Both observed and modelled results in Figure 4b show the same gradual decline in sediment concentration with distance from the river mouth, although the modelled concentrations are systematically too high. The fit to observational data in both plots is acceptable, and justifies the use, for the present, of a single constituent sediment model. The comparison of the modelled and observed contaminant concentrations in the Niagara River plume was a principal part of the work described in Stepien *et al.*, (1987). Of the three observational periods in 1983, one data set was set aside for calibration of the model. The major parameters available for calibration were the sinking rate of sediment and the partition coefficient. The partition coefficient was determined analytically to be 0.087 mg L^{-1} for 1,2,3,4-TeCb and 0.067 mg L^{-1} for 1,2,4-TCB. The sediment sinking rate was determined by comparing the modelled suspended sediment distribution with that observed in the plume. Three values were tested: 1, 2, and 3 m d^{-1}. The accuracy of the modelled concentration fields, in terms of standard error, was not particularly sensitive to the three values of sinking rate, being 1.07, 1.05, and 1.12 ng/L, respectively. On the basis of these values, a sinking rate of 2 m d^{-1} was used. Figure 5 is typical of the calibration achieved with this setting. In these diagrams, the instantaneous values from the model at 1700 on October 4 (contours) are compared with the pseudo-synoptic sampled values (circles), obtained over the period from 14:50 to 21:00. The spatial patterns are similar, as are the levels. The standard deviation between computed and observed values was 1.5, 0.7 and 0.7 ng L^{-1} for total, dissolved and particulate concentrations, and 0.7 mg L^{-1} for suspended sediment concentration, well within the uncertainties of the observed data.

6 STRAIT OF GEORGIA SCENARIOS

Stepien *et al.* (1987) provide a number of examples of flow fields and contaminant distributions for the Niagara River plume. In this section, the

modelled spatial distributions of the contaminant and sediment plumes for the Fraser River plume will be examined in order to provide an indication of the mechanisms of contaminant transport throughout the Strait of Georgia. Because the calibration of the sediment transport model was done for the high flow rates of late May, it is likely that the model results will be reasonably valid as long as conditions do not differ markedly from the calibration period. May 20 was selected as representative of this period.

Figure 6 presents the wind time-series at Sand Heads for the months of May 1988 and June 1988. Generally speaking, both months were relatively calm, without either particularly strong winds or extended periods of persistent winds. However, a reasonably strong northwest wind on June 3 provided an opportunity to examine the effects of stronger winds on contaminant distributions.

May 20, 1988

The modelled distribution of contaminant and sediment on May 20 has been plotted to determine the spatial extent and temporal variations of these scalars under relatively high river discharge conditions and also to examine the effectiveness of sediment adsorption as a mechanism for removing contaminant from the water column. Thus, two runs were done, one in which the contaminant was allowed to adsorb onto sediment as given by equations (1) and (2), and another run in which the contaminant was assumed to occur totally in the dissolved phase, i.e., the partition coefficient was set to zero.

Figure 7 shows the tidal elevation at Point Atkinson for May 20, and the preceding and following 6 hours. Arrow heads show the times of vector plots, and squares show the times of surface property contours. In order to describe the flow characteristics of the Fraser River plume, Figures 8, 9, and 10 show representative current fields for an ebb, for low tide, and for a flood tide respectively. The ebb tide plot, Figure 8, shows a strong ebb flow south of the river, but north of the river currents are considerably weaker, and much of the flow is directed in the northward, flood direction. The low tide plot, Figure 9, shows the jet of water issuing from the Fraser River being deflected by the Gulf Islands and by a flow coming from the north along the Vancouver Island shore. A front forms between these two water masses, as indicated by a shear line about 4 grid cells (8 km) off the Vancouver Island shore. The flood velocity field, Figure 10, shows the strong flood tidal flow south of the river jet and a well-defined jet moving from the river mouth to the Gulf Islands and then back to the Sechelt shore. As noted in Figure 9, the flow near the Vancouver Island shore, north of the river, differs considerably from the flow in the main part of the Strait, in this case being directed toward Vancouver Island.

Figures 11 and 12 show the upper layer salinity field calculated by the model at the times of the Kostaschuk *et al.* (1989) survey. Figure 11 corresponds

to high water, and indicates that in the area south of the river, the plume has been compressed, as shown by the large salinity gradient there. North of the river mouth, the plume extends as far as the southern tip of Texada Island. Figure 12 corresponds to low water, and shows the plume has expanded to the south, as a result of the preceding ebb tide. North of the river, the salinity fields of Figures 11 and 12 do not differ substantially. For the wind and tide conditions prevailing on May 20, the currents north of the river tend to be directed primarily northeast, along the axis of the Strait, and do not undergo a significant reversal during the ebbing tide, as shown for example in Figure 8. Consequently, the salinity distribution north of the river mouth tends to be nearly stationary. A strong northwest wind would presumably change this situation.

Figures 13 and 14 show the corresponding distribution of suspended sediment, the contoured values being concentration in mg L^{-1}. The distributions are quite similar to the salinity distributions. This similarity is not surprising, as both scalars are advected by the same velocity field, and both undergo losses, through vertical mixing in the case of salinity, and through both vertical mixing and settling in the case of sediment. Figure 14 shows considerably higher concentrations of sediment near the river mouth, a consequence of the tidal variation in sediment supply given by equation (6).

Figure 15 plots the time series of modelled suspended sediment concentrations at the river mouth, and at 4.5 and 9.0 km from the river mouth, from 18:00 PST May 19 to 06:00 PST May 21. These positions are plotted on Figure 13. Also plotted is the time series of river discharge used as a boundary condition for the model. The rapid decrease in concentration away from the river during times of high sediment discharge is apparent in these time series. Also present, but not readily apparent, is the phase delay of the maxima of concentration, which occurs later in time with increasing distance from the river mouth. This phase delay is associated with the time for the sediment maximum to propagate away from the river mouth. The sediment time series at the two outer stations in the Strait also display a temporal asymmetry, the rising part of the curve being steeper than the falling. This feature indicates the manner in which GF4 simulates the propagation of a front through the system: the front is present, but not well-resolved.

Contaminant Concentrations With Sediment Adsorption

Figures 16 and 17 plot contours of contaminant concentration, for the same times as the sediment contour plots in the previous section, and for a partition coefficient of 0.077 mg L^{-1}. The contaminant concentration was set at 100 mg L^{-1} at the river mouth, so that contoured values represent the percentage of the river concentration. The distribution of contaminant follows a similar pattern to the sediment and freshwater distributions, because again, similar processes are acting.

Figure 18 is a time series of contaminant concentration at distances of 1.4, 4.5 and 9.0 km from the river mouth. These locations are shown on Figure 16. The river mouth time-series is not plotted, as it remains steady at a value of 100 mg L^{-1}. The rapid decline of concentration near the river mouth can be observed in this plot, as well as the smaller rate of decline farther away.

Contaminant Concentrations Without Sediment Adsorption

In order to demonstrate the effect of the adsorption of contaminant on sediment, the above simulation was repeated, but with the partition coefficient set to 0.0 L mg^{-1}. Figures 19 and 20 plot the contaminant concentration at the same times as the previous section. Comparison with Figures 16 and 17 shows that the contaminant levels are much higher in the non-adsorbing case.

Figure 21 is a time-series plot of contaminant concentration, from 18:00 PST May 19 to 6:00 PST, May 21, at distances of 1.4, 4.5 and 9.0 km from the river mouth. These locations are shown on Figure 19. Figures 18 and 21 indicate that the ratios of concentrations between the two simulations, with and without adsorption, is about 5 to 1 for the station 9 km from the river mouth. This ratio indicates the large role which sediment adsorption plays in the distribution of contaminants in the Strait of Georgia: concentrations in surface waters are much lower than would be the case if sediment adsorption were not present. Furthermore, the distribution of contaminant can be seen to involve the entire water column, and the contaminant-laden sediment must be tracked all the way to the sea-floor if one wants to model the ultimate fate of the contaminant.

June 2-4, 1988

Typical satellite images of the Strait of Georgia, such as Figure 4 of Crean (1977), show the Fraser River plume being swept southward as a result of strong northwest winds. As indicated in Figure 6, during the simulation discussed here there were no periods of particularly strong northwest winds that could move the plume significantly southward. However, there were a few periods of persistent south and southeasterly winds followed by persistent northwesterly winds such as June 2 to June 4, that illustrate the influence of wind forcing on water motion and contaminant distribution.

June 1 and 2 were characterized by southeasterly winds, followed on June 3 by relatively strong northwesterly winds with peak speeds of 9 m s^{-1} at Sand Heads. Figures 22 and 23 are plots of the contaminant concentrations at 0:00 PST on June 2 and June 4 respectively . During the period of southeasterly winds (Figure 6) there is a slight intensification of contaminant concentration along the Sechelt coast that is advected laterally into the central part of the Strait under the influence of the subsequent northwesterly winds (Figure 23). Figure 23 also reveals a decrease

in concentrations that is primarily due to the increased wind mixing during the period of stronger northwest winds. This characteristic can be seen, for example, in the central part of the plume adjacent to the mouth of Howe Sound where concentrations are substantially lower on June 4 than on either June 2 (Figure 22) or May 20 (Figures 16 and 17).

Figure 24 is a plot of the surface current field at 0:00 PST on June 4, which is almost identical in tide phase to Figure 25, corresponding to 00:00 PST May 20. The southerly set to the currents on June 4 due to the northwesterly winds, and their increase in speed, compared to conditions on May 20, is apparent, particularly in the southern part of the Strait.

7 CONCLUSIONS AND RECOMMENDATIONS

The modelling and observational program for the Niagara River plume demonstrated that the proposed contaminant model, including the effects of partitioning and sediment settling, offered a reasonable description of the contaminant transport processes near the mouth of the river. The modelling work in the Strait of Georgia extended that process by examining the fate in the presence of much higher sediment concentrations and by examining the process over much longer time and space scales.

Summary of Strait of Georgia Modelling Results

The preliminary calculations reported here, using a coupled hydrodynamic and transport-diffusion model for the Fraser River and Strait of Georgia, have provided intuitively reasonable results using salinity and sediment as scalar tracers. The sediment distribution agrees qualitatively with satellite imagery, and with a limited set of *in situ* measurements. The salinity distribution has also been shown in earlier work (Stronach *et al.*, 1988) to agree with observed distributions. Thus, the dynamics of scalar transport in the Strait of Georgia appear to be correctly modelled.

Applications of the model in this study have also shown several important features that must be considered in contaminant modelling in general, and for the Strait of Georgia in particular:

1. The geographic extent of relatively high concentrations of contaminant is quite large, extending up to Texada Island before a 1% dilution from river values is achieved; consequently the model must include the entire Straits of Georgia and Juan de Fuca.

2. Adsorption of contaminants onto sediment is a major controlling factor; however, data on contaminant partitioning amongst the grain sizes and

sediment types occurring in the Fraser River, in the presence of saline water, are not presently available to the degree required for detailed modelling, and this represents a serious data gap.

3. Even small wind events can change the contaminant distribution significantly, and hence wind forcing becomes an important factor in contaminant modelling.

Recommended Modelling Improvements

The fate of contaminants in the Strait of Georgia originating from the Fraser River is an important issue, and a reliable numerical model is an essential tool both for management decisions and for sampling and monitoring program design. Based on the degree of success achieved with limited resources in this study, and the work of Stepien *et al.* (1987), development of a three-dimensional contaminant dispersion model for the Strait of Georgia and Juan de Fuca is strongly recommended. Such a model would provide major improvements in the management of contaminant loads in the Fraser Estuary, and in understanding the distribution and fate of contaminants in the Strait of Georgia. For example, the model would provide information on:

1. sites of contaminant accumulation;

2. the distribution of Fraser-derived contaminants relative to the distribution of contaminants from other point sources in the Strait;

3. the long-term effects of particular water quality objectives (Swain and Holms, 1985).

The elements to construct and calibrate such a model are reviewed briefly below.

A Fully Three-dimensional Hydrodynamic Model

The model used in this study, GF4, deals only with currents in the top three to five meters of the water column. Contaminants enter other parts of the water column, either by mixing downward, or by attaching to sediment and settling out. Thus, the hydrodynamic model must extend through the entire water column. Presently the most appropriate hydrodynamic model is GF9 (Stronach, 1992). GF9 is a fully three-dimensional model that has been carefully calibrated to the dynamics of the Straits of Georgia and Juan de Fuca. It provides reliable velocity fields using fixed levels to describe the vertical variation of properties, with a dynamic interface to separate the surface layer from the underlying waters, similar to the GF4 formulation. This dynamic formulation for the uppermost layer

is particularly appropriate for the strong density stratification characterizing the Fraser River plume.

A Complete Sediment Balance Model, Verified Against Measurements

In view of the importance of river-borne sediments to the fate of contaminants, a sediment balance model incorporating a range of grain sizes and fall velocities is required. This model would eliminate the ad hoc formula in the present model relating fall velocity to sediment concentration in favour of a more physically correct distribution of fall velocities related to grain size.

The sediment balance model must be calibrated and verified against observed sediment distributions in different seasons. The verification should use a combination of remotely-sensed imagery, to provide complete spatial coverage, and *in situ* measurements using high-resolution nephelometry and water samples to give detailed date in areas of particular interest. Instruments such as a nephelometer operated in towed and profiling modes could be used to give three-dimensional fields for quantifying the satellite image data. The imagery and concentrations fields would then be compared with model output. As Carey and Hart (1988) point out, it is often difficult to verify a contaminant model directly because of logistical considerations for sampling, the expense of analyses, and the episodic nature of the contaminant inputs. However, verifying the sediment module provides a good means of verifying many of the processes which enter into the contaminant model.

Improved Models of Contaminant Adsorption

Numerical experiments in this study have demonstrated the sensitivity of contaminant fate to sediment adsorption assumptions. Physical-chemical measurements will be required to refine and calibrate the contaminant adsorption model by grain size and sediment type, and to understand the effects of salt water on the process.

Improved Resolution of the Fraser River Mouth

Roberts and Sturgeon Banks are biologically important regions. The pathways of contaminants onto Roberts and Sturgeon Banks consist primarily of recirculation from the Main Arm discharge and fluxes from localized sources such as Canoe Pass, Middle Arm, various small gaps in the jetties south of the Main Arm, and through the lateral movement of small amounts of the Main Arm flow southward across Roberts Bank.

GF4 considers only two of these sources: the South Arm and the North Arm. The significance of the other, smaller distributary mouths as sources of contaminant has not been addressed. Their importance could be assessed by a combination of field studies and the development of a high resolution sub-model for the Roberts and Sturgeon Bank areas.

Improved boundary condition data for contaminant and suspended sediment

Additional data are required for the rate of supply of suspended sediment at the river mouth, taking tidal fluctuations into account. Some information on the fluxes of contaminants could be obtained from the contaminant transport model developed for the Fraser River by Lam *et al.* (1988). In fact, the Lam *et al.* Fraser River model could be dynamically linked to the Strait of Georgia model, including the high-resolution banks sub-model, to provide a complete Fraser Estuary-Strait of Georgia contaminant transport and fate model.

Quantification of Other Sink Mechanisms

Aside from sedimentation, processes that act as sinks for contaminants, and the availability of data to describe them, were not identified in this study. Additional work is required to identify such processes and models for them.

8 ACKNOWLEDGEMENTS

The first author was supported by contracts from Environment Canada and from the Department of Fisheries and Oceans.

REFERENCES

Ages, A. 1988. The salinity intrusion in the Fraser River: time series of salinities, temperatures and currents 1978, 1979. Can. Data Rep. Hydrogr. Ocean Sc. 66.

Ages, A. 1979. The salinity intrusion in the Fraser River: salinity, temperature and current observations, 1976, 1977. Pac. Mar. Sci. Rep. 79-14.

Allan, R.J., A. Mudroch and A. Sudar. 1983. An introduction to the Niagara River/Lake Ontario pollution problem. J. Great Lakes Res. 9: 111-117.

Anonymous. 1981. Environmental impact statement of proposed improvements to the Fraser River shipping channel. Prepared for Public Works Canada by Beak Consultants Ltd., Vancouver, B.C., Oct. 1981. 202 pp.

Carey, J.H. and J.H. Hart. 1988. Sources of chlorophenolic compounds to the Fraser River Estuary. Water Poll. Research J. Canada 23: 55-68.

Crean, P.B. 1978. A numerical model of tides between Vancouver Island and the mainland and its relation to studies of estuarine circulation. In: Hydrodynamics of Estuaries and Fjords, Proceedings of the 9th International Liege Colloquium on Ocean Hydrodynamics. J.C.J. Nihoul [Ed.]. Elsevier, Amsterdam, 546 pp.

Crean, P.B., J.A. Stronach and T.S. Murty. 1988. Salt and freshwater exchange on Roberts Bank, British Columbia. Water Poll. Research J. Canada 23: 160-178.

Elder, V.A., B.L. Proctor and R.A. Hites. 1981. Organic compounds near dump sites in Niagara Falls, New York. Environ. Sci. Technol. 15: 1237-1243.

Frank, R., R.L. Thomas, M. Holdrinet, A.L.W. Kemp and M.E. Braun. 1979. Organochlorine insecticides and PCBs in surficial sediments (1968) and sediment cores (1979) from Lake Ontario. J. Great Lakes Res. 5: 18-27.

Hodgins, D.O. 1974. Salinity Intrusion in the Fraser River, British Columbia. Ph.D. Thesis, University of British Columbia, 147 pp.

Kostaschuk, R.A., B.A. Stephan and J.L. Luternauer. 1989. Sediment dynamics and implications for submarine landslides at the mouth of the Fraser River, British Columbia. In: Current Research, Part E, Geological Survey of Canada, Paper 89-1E, pp 207-212.

Lam, D.C.L. 1978. Simulation of water circulation and chloride transports in Lake Superior for summer 1973. J. Great Lakes Res. 4: 343-349.

Lam, D.C.L., C.R. Murthy and R.B. Simpson. 1984. Effluent transport and diffusion models for the coastal zone. Lecture Note Series on Coastal and Estuarine Studies, Vol. 5, Springer-Verlag, New York, 168 pp.

Lam, D.C.L., R.C. McCrimmon, J.H. Carey and C.R. Murthy. 1988. Modelling the transport and pathways or tetrachlorophenol in the Fraser River. Water Poll. Research J. Canada 23:141-159.

Masse, A.K. and C.R. Murthy. 1990. Observations of the Niagara River thermal plume (Lake Ontario, North America). J. Geophys. Res. 95: 16,097-16,1209.

Milliman, J.D. 1980. Sedimentation in the Fraser River and its Estuary, Southwestern British Columbia (Canada). Estuarine and Coastal Marine Science 10: 609-633.

Murthy, C.R. and K.C. Miners. 1989. Mixing characteristics of the Niagara River plume in Lake Ontario. Water Poll. Research J. Canada 24:144-162.

Murthy, C.R., T.J. Simons and D.C.L. Lam. 1986. Dynamic and transport modelling of the Niagara River Plume in Lake Ontario. Rapp. P-v. Reun. Cons. int. Explor. Mer 186: 150-164.

Niagara River Toxics Committee (NRTC). 1984. U.S.-Canada Niagara River Toxics Committee Report. Inland Waters Directorate, Ontario Region, Burlington, Ontario.

Pharo, C.H. and W.C. Barnes. 1976. Distribution of surficial sediments of the central southern Strait of Georgia, British Columbia. Can. J. Earth Sci. 13: 684-696.

Simons, T.J. 1980. Circulation models of lakes and inland seas. Can.Bull. Fish. Aquat. Sci. Vol. 203, 146 pp.

Stepien, I., D.C. Lam, C.R. Murthy, M.E. Fox and J. Carey. 1987. Modelling of toxic contaminants in the Niagara River plume in Lake Ontario. J. Great Lakes Res. 13: 250-263.

Stronach, J.A. 1992. GF9: A hybrid upper layer/three-dimensional model for the Georgia/Fuca system. Report prepared for Fisheries and Oceans Canada by Seaconsult Marine Research Ltd., Vancouver, B.C.

Stronach, J.A., P.B. Crean and T.S. Murty. 1988. Mathematical modelling of the Fraser River plume. Water Poll. Research J. Canada. 23: 179-212.

Warry, D. and C.H. Chau. 1981. Organic contaminants in suspended sediments of the Niagara River. J. Great Lakes Res. 7:

394-403.

Zalesak, S.T. 1979. Fully multidimensional flux-corrected transport algorithms for fluids. J. Comput. Phys. 31: 35-362.

LIST OF FIGURES

indicate stations that are 4.5 and 9 km from the river mouth for which time series are plotted in Figure 15.

Figure 14: Upper layer suspended sediment concentration field predicted by GF4 for 20:00 PST on May 20, 1988, corresponding to high water. Units of concentration are mg L^{-1}.

Figure 15: Time-series of suspended sediment concentrations at the river mouth and at 4.5 and 9.0 km downstream from the river mouth over the period from 18:00 PST on May 19, 1988 to 06:00 PST on May 21, 1988, as predicted by GF4.

Figure 16: Upper layer contaminant concentration field predicted by GF4 for 07:00 PST on May 20, 1988, corresponding to high water. Adsorption of contaminant onto sediment is incorporated into the calculation. Units of concentration are % of river mouth value. The solid squares indicate stations that are 1.4, 4.5 and 9 km from the river mouth for which time series are plotted in Figure 18.

Figure 17: Upper layer contaminant concentration field predicted by GF4 for 14:00 PST on May 20, 1988, corresponding to low water. Adsorption of contaminant onto sediment is incorporated into the calculation. Units of concentration are % of river mouth value.

Figure 18: Time-series of contaminant concentrations at distances of 1.4, 4.5 and 9.0 km downstream from the river mouth over the period from 18:00 PST on May 19, 1988 to 06:00 PST on May 21, 1988, as predicted by GF4. Adsorption of contaminant onto the sediment is incorporated in the calculations.

Figure 19: Upper layer contaminant concentration field predicted by GF4 for 07:00 PST on May 20, 1988, corresponding to high water. Adsorption of contaminant onto sediment is not incorporated into the calculation. Units of concentration are % of river mouth value. The solid squares indicate stations that are 1.4, 4.5 and 9 km from the river mouth for which time series are plotted in Figure 21.

Figure 20: Upper layer contaminant concentration field predicted by GF4 for 14:00 PST on May 20, 1988, corresponding to low water. Adsorption of contaminant onto sediment is not incorporated into the calculation. Units of concentration are % of river mouth value.

Figure 21: Time-series of contaminant concentrations at distances of 1.4, 4.5 and 9.0 km downstream from the river mouth over the period from 18:00 PST on May 19, 1988 to 06:00 PST on May 21, 1988, as

predicted by GF4. Adsorption of contaminant onto the sediment is not incorporated in the calculations.

Figure 22: Upper layer contaminant concentration field predicted by GF4 for 00:00 PST on June 2, 1988. Adsorption of contaminant onto sediment is incorporated into the calculation. Southeasterly winds were prevailing at the time. Units of concentration are % of river mouth value.

Figure 23: Upper layer contaminant concentration field predicted by GF4 for 00:00 PST on June 4, 1988. Adsorption of contaminant onto sediment is incorporated into the calculation. Northwesterly winds were prevailing at the time. Units of concentration are % of river mouth value.

Figure 24: Surface current field predicted by GF4 for 00:00 PSTon June 4, 1988.

Figure 25: Surface current field predicted by GF4 for 00:00 PST on May 20, 1988.

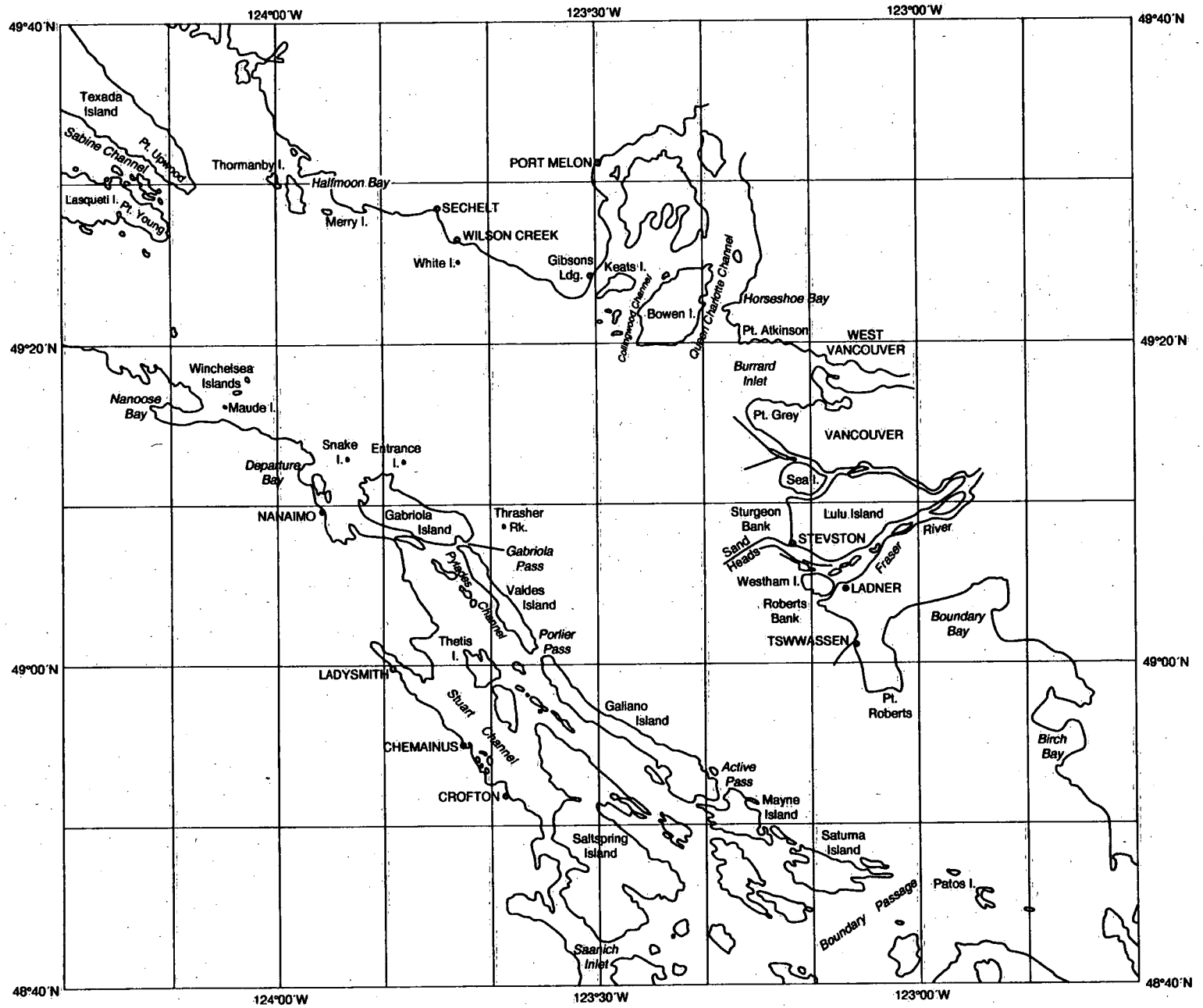

Figure 1: Map of the southern Strait of Georgia showing the study area.

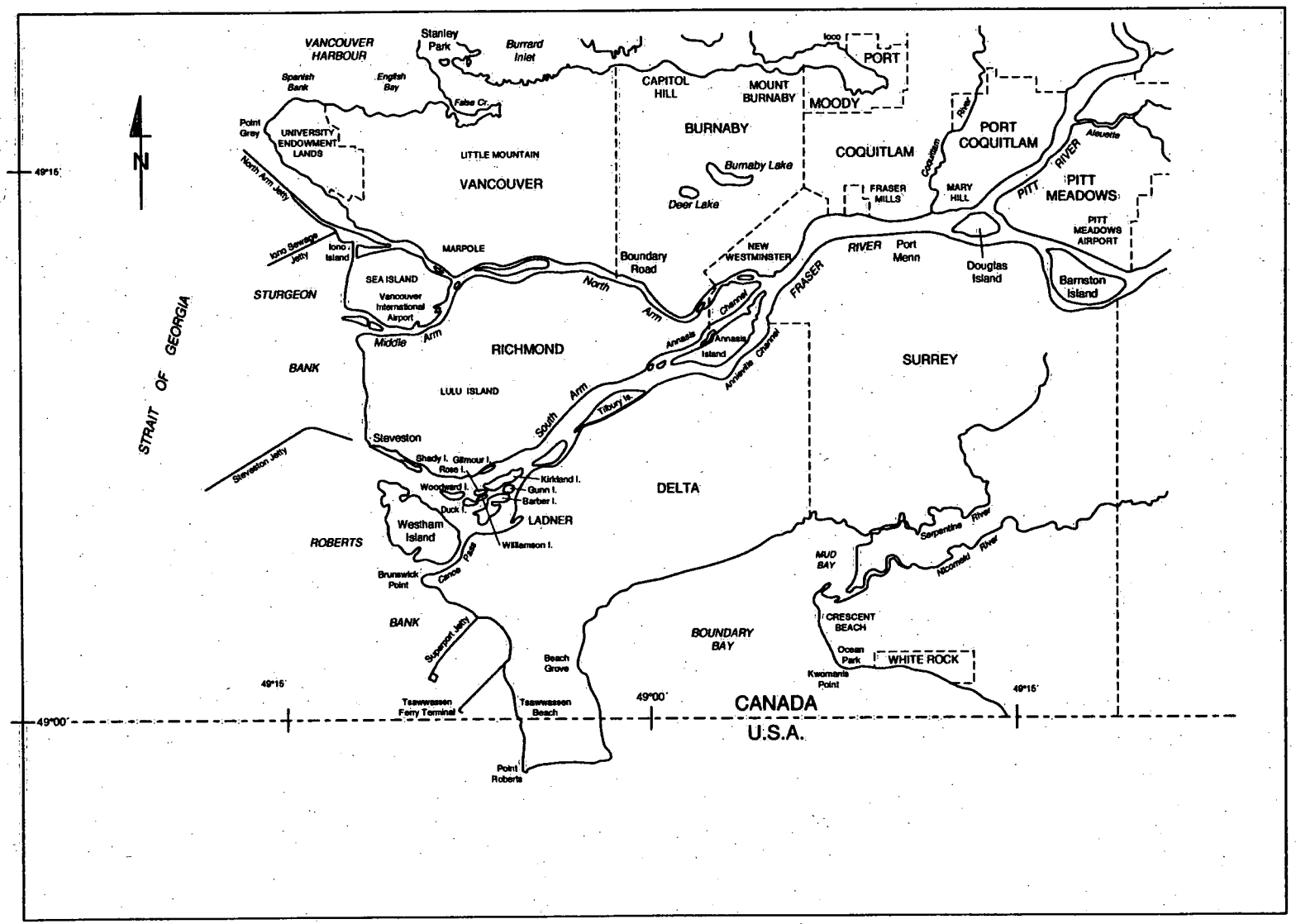

Figure 2: Map of the Fraser Estuary.

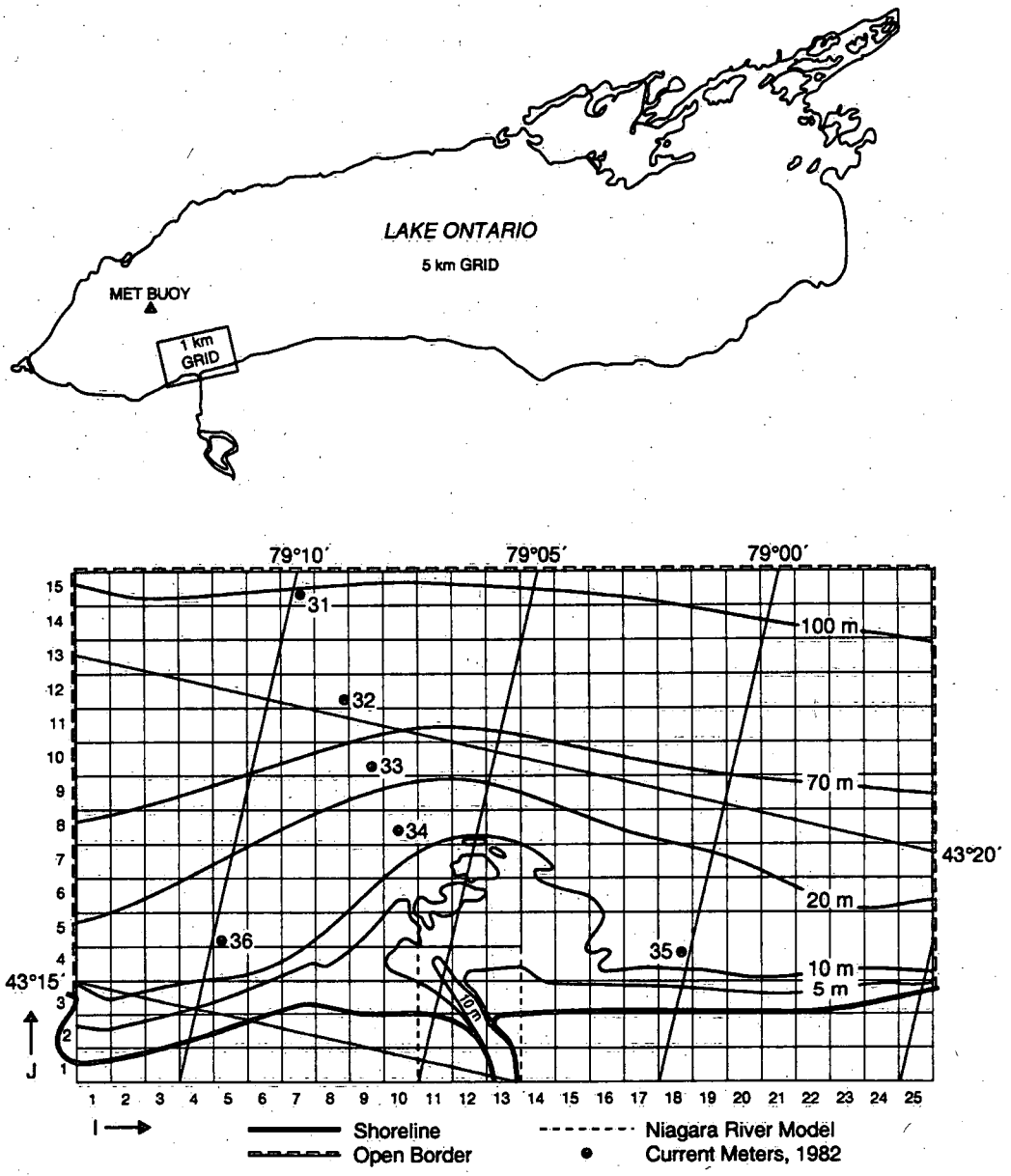

Figure 3: Map of the Niagara River and Lake Ontario showing the 1 km grid.

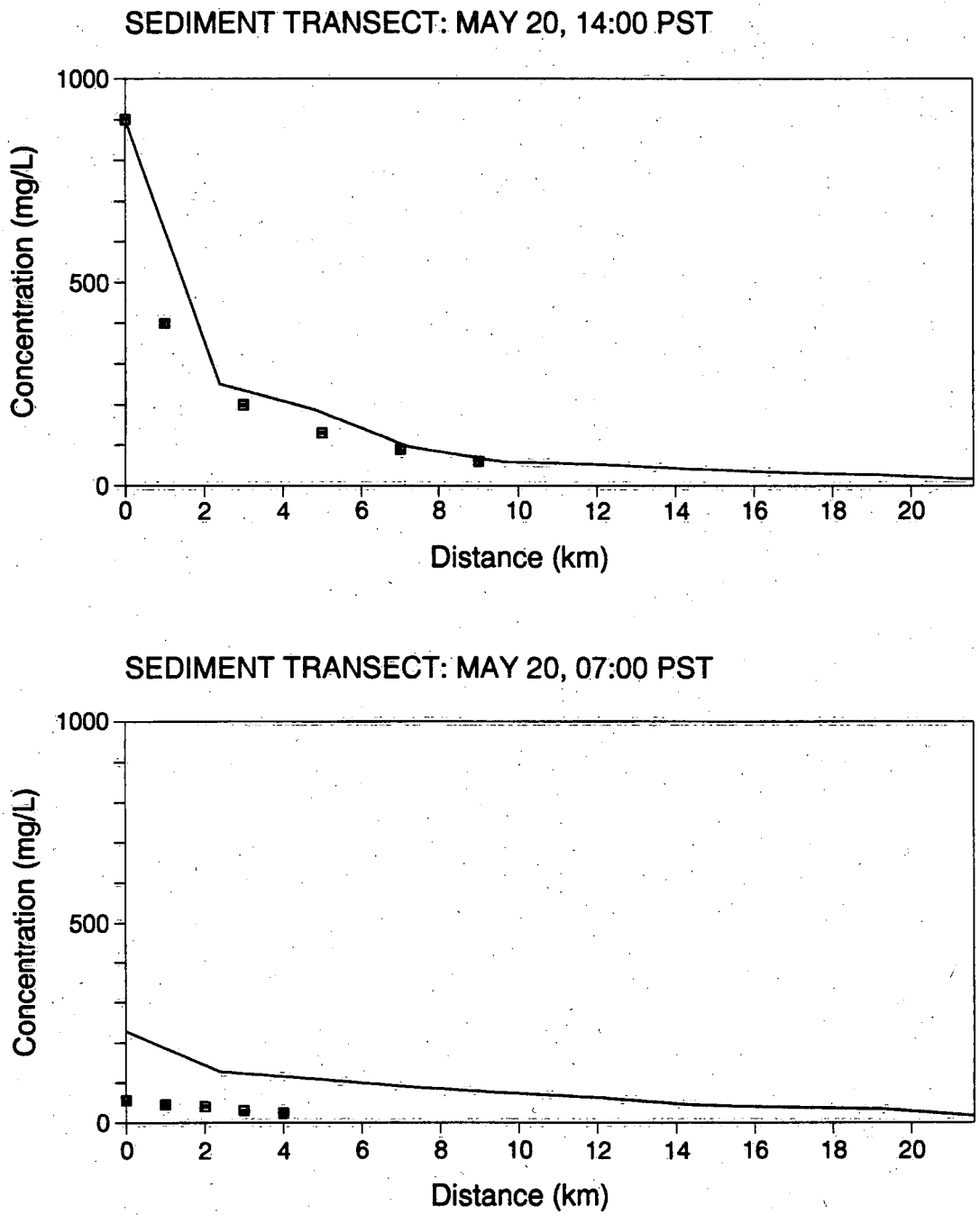

Figure 4: Suspended sediment transect on May 20, 1988, at a stage of the tide corresponding to maximum river flow and sediment concentration (a), and at a stage of the tide corresponding to minimum river flow and concentration. Observed concentrations (from Kostaschuk et al., 1988) are indicated by solid squares, modelled concentrations by a continuous line.

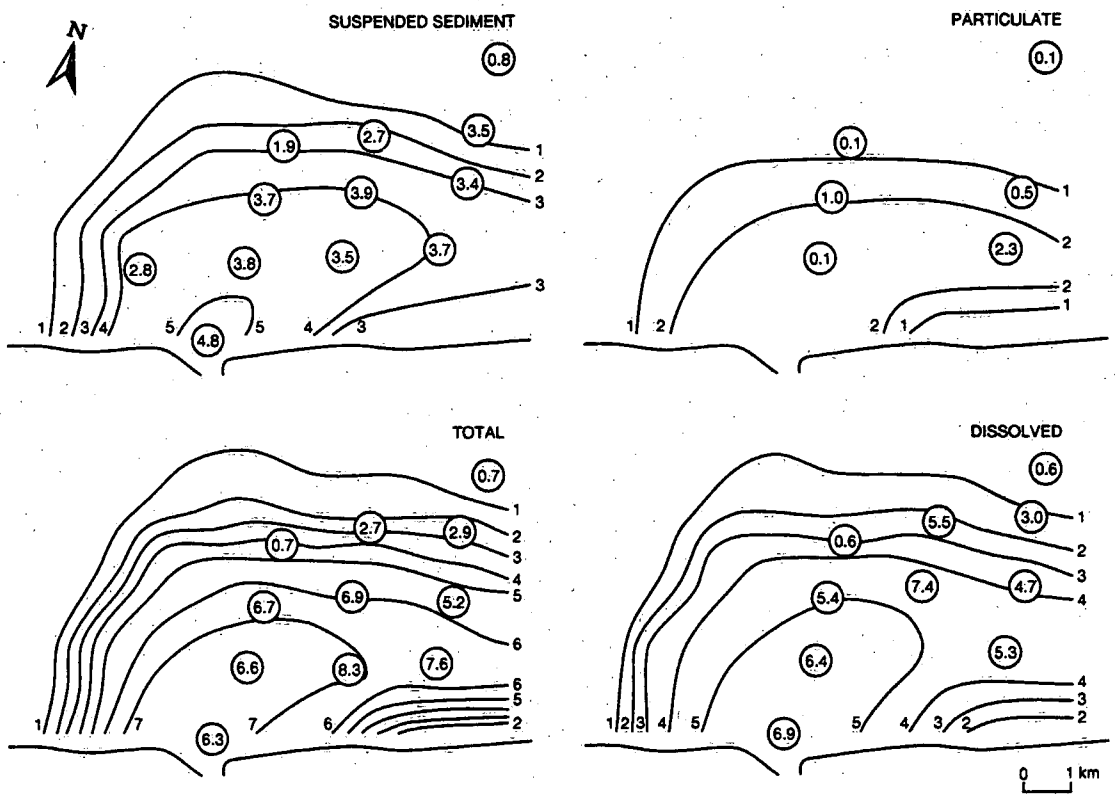

Figure 5: Total and fractional 1,2,3,4-TeCB concentration (ng L^{-1}) and suspended sediment concentration (mg L^{-1}). The observed values (circles) were sampled between 1450 and 2100 GMT; the computed values (contours) were for 1700 GMT, 4 October, 1983.

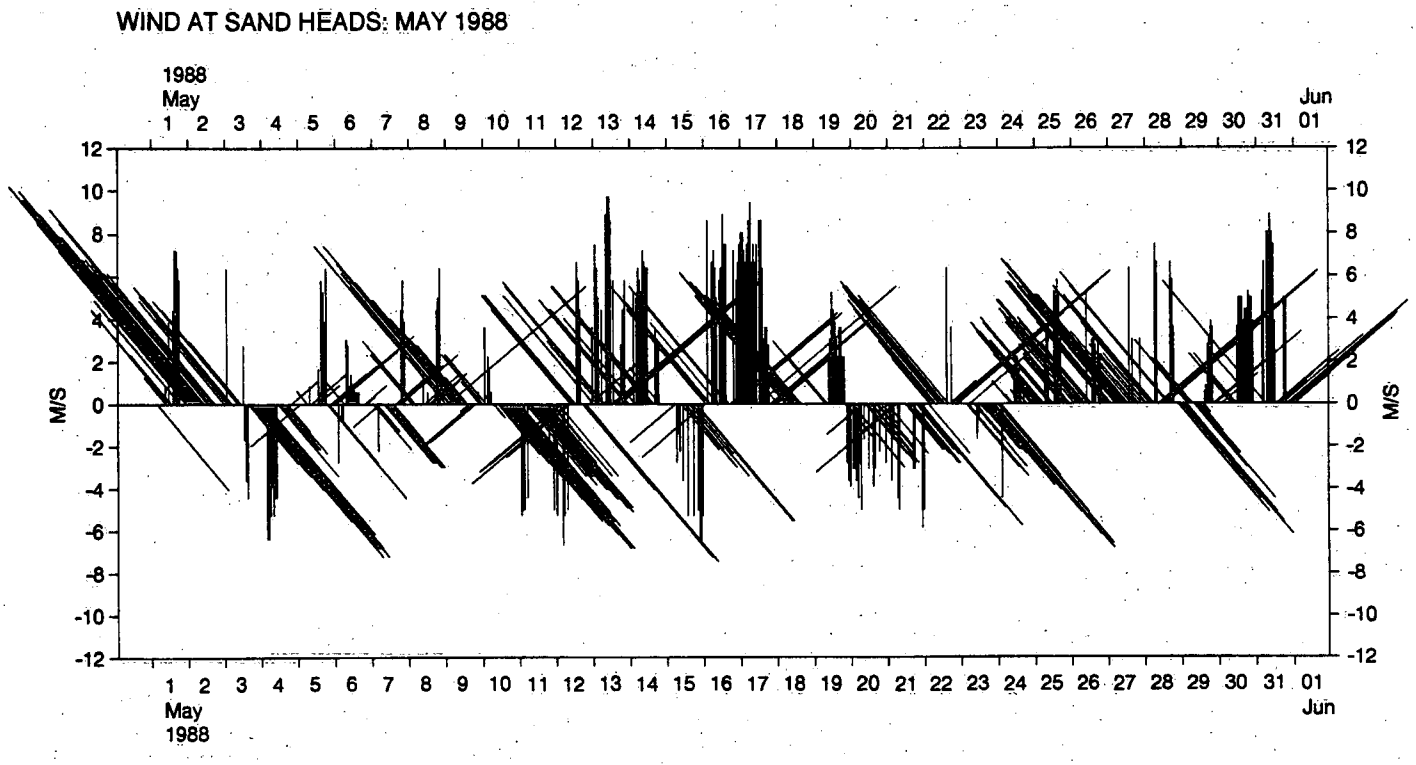

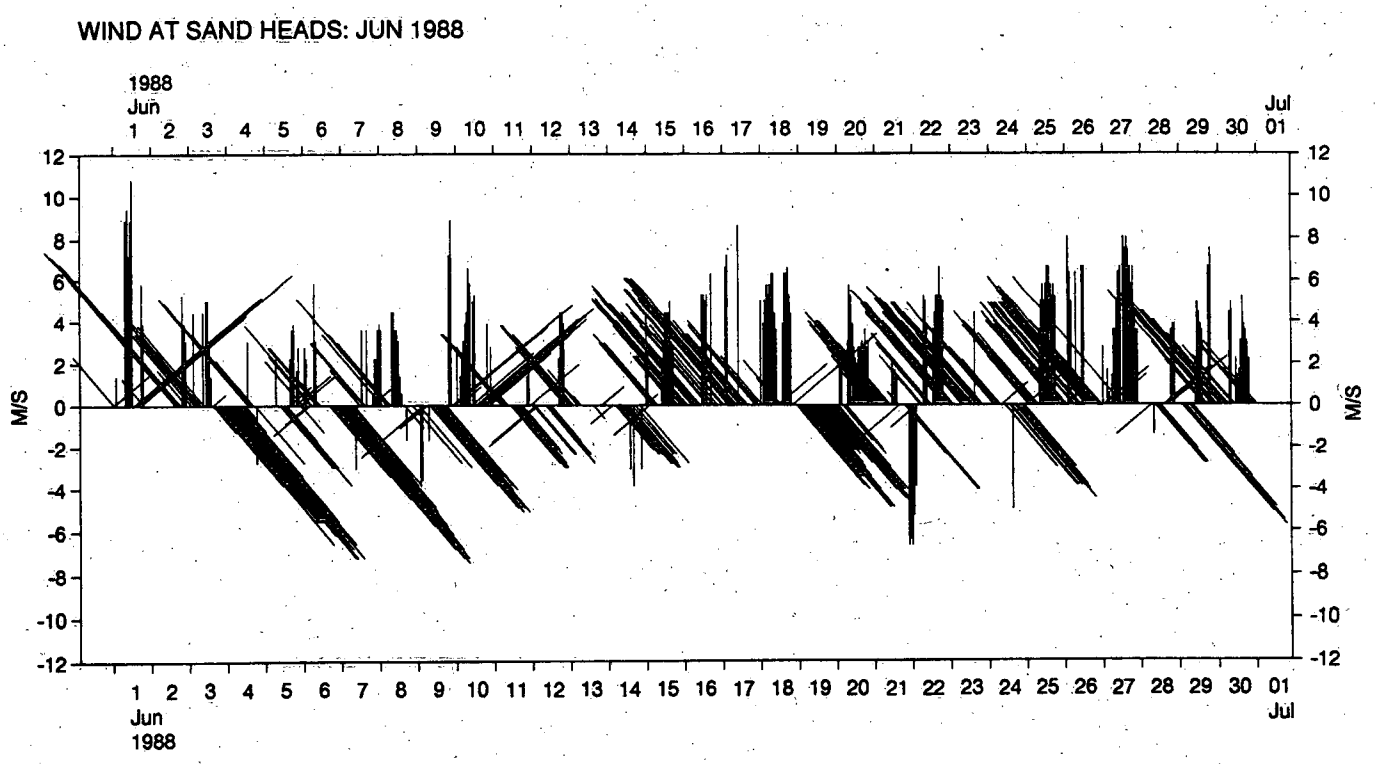

Figure 6: Winds at Sand Head for May and June, 1988.

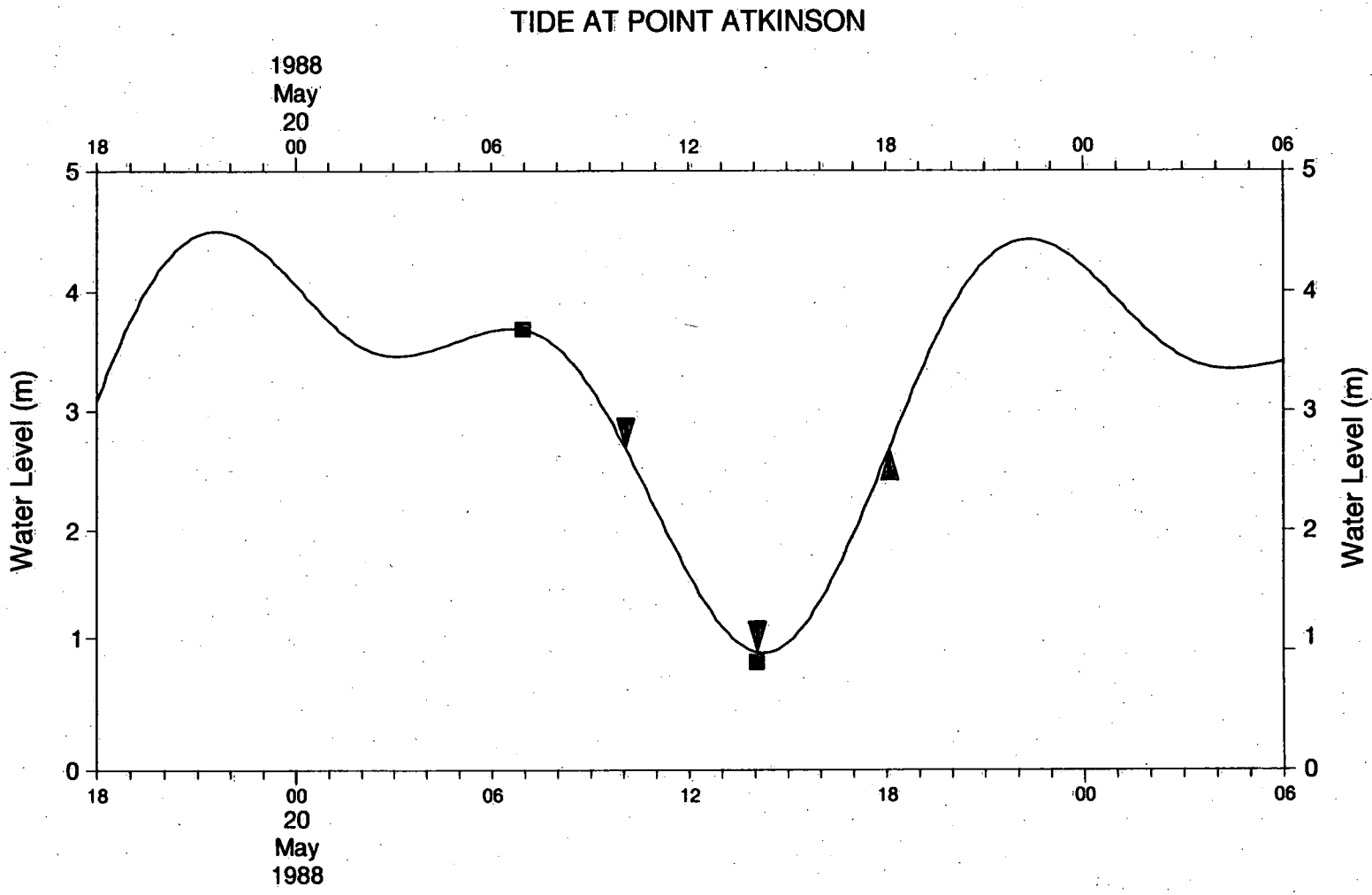

Figure 7: Tidal elevations at Point Atkinson from 18:00 PST on May 19, 1988 to 06:00 PST on May 21, 1988. Arrow head show the times of vector plots, and squares show the times of surface property contour plots.

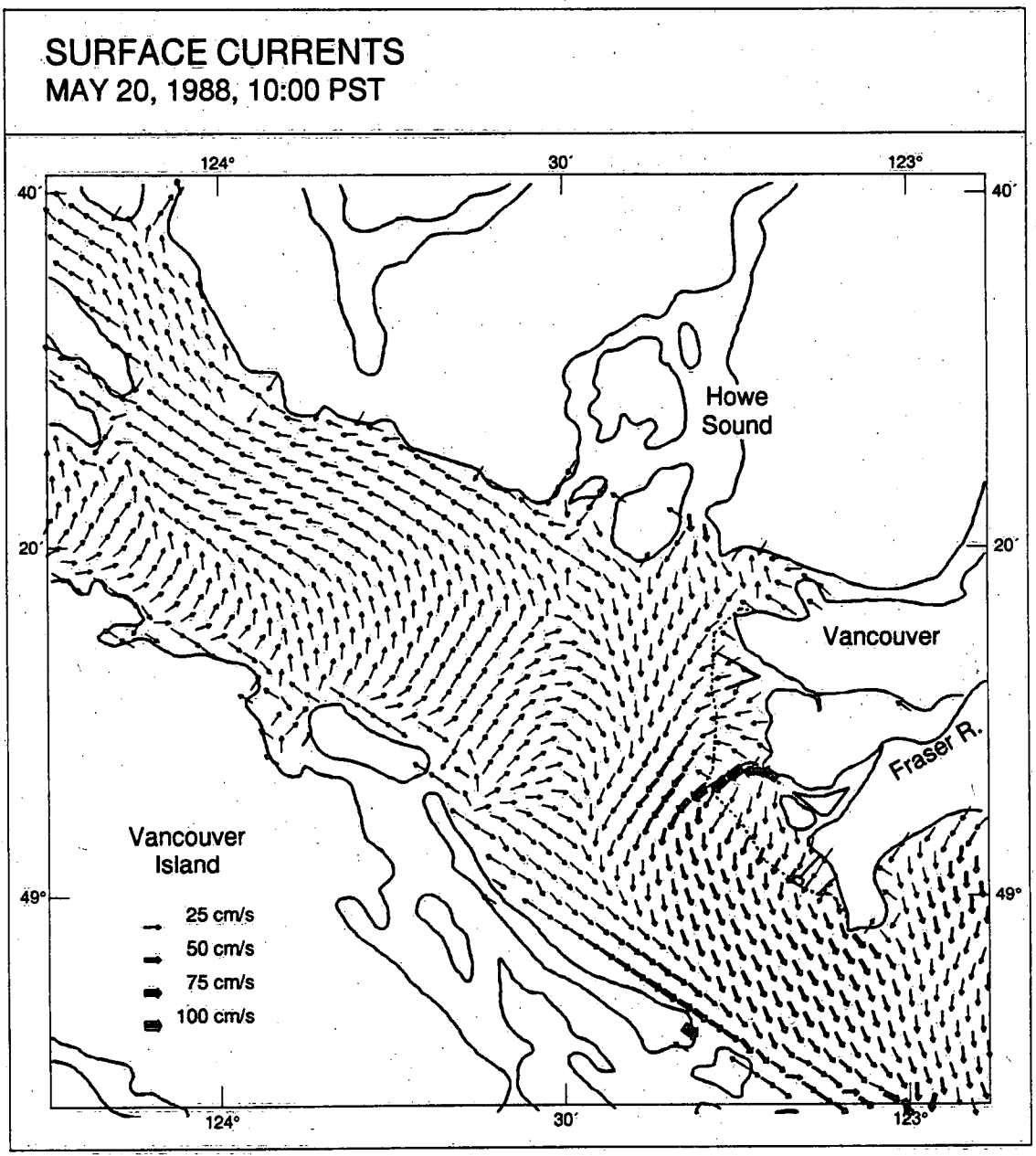

Figure 8: Surface current field predicted by GF4 for 10:00 PST on May 20, 1988, corresponding to an ebbing tide.

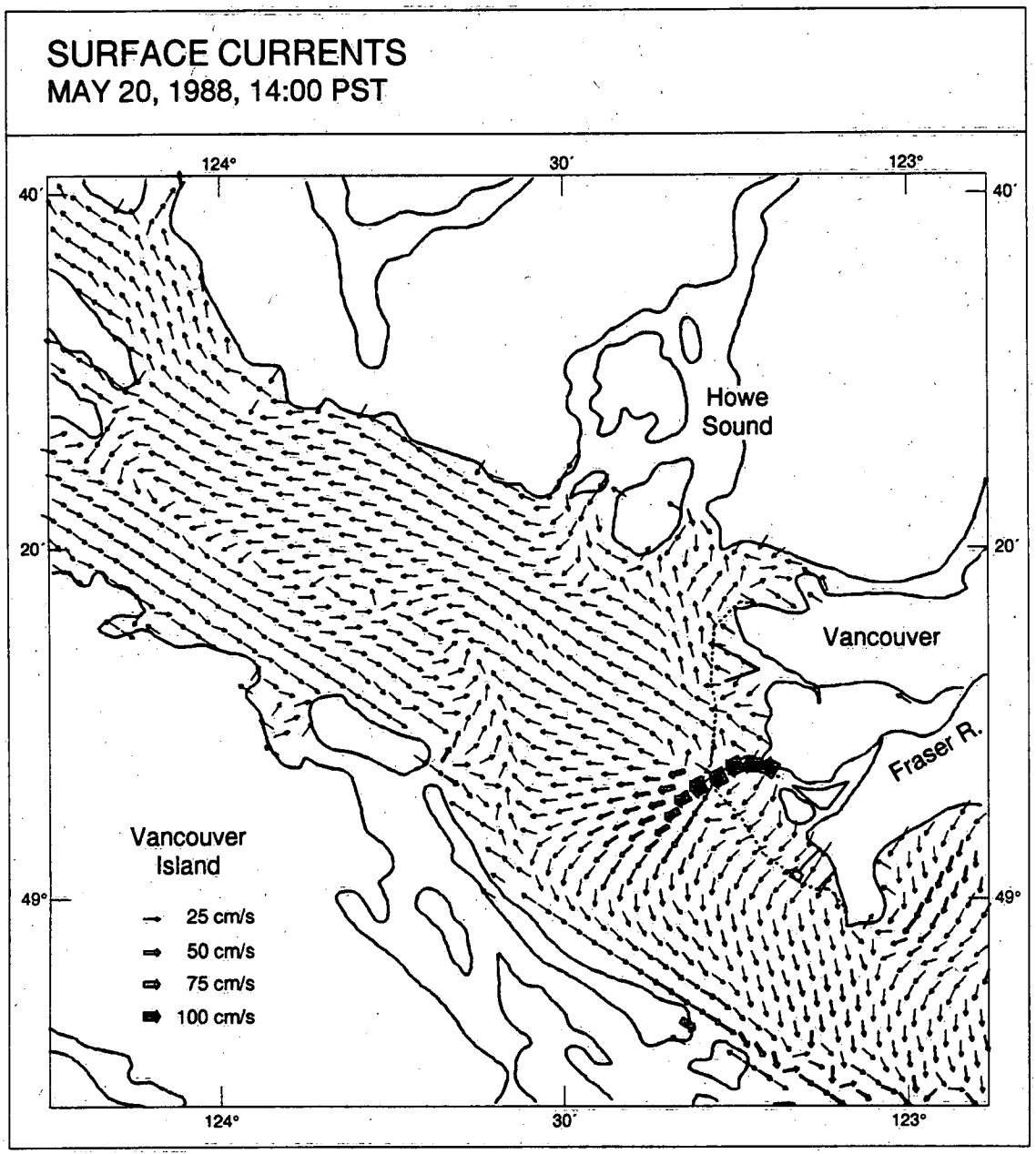

Figure 9: Surface current field predicted by GF4 for 14:00 PST on May 20, 1988, corresponding to low water.

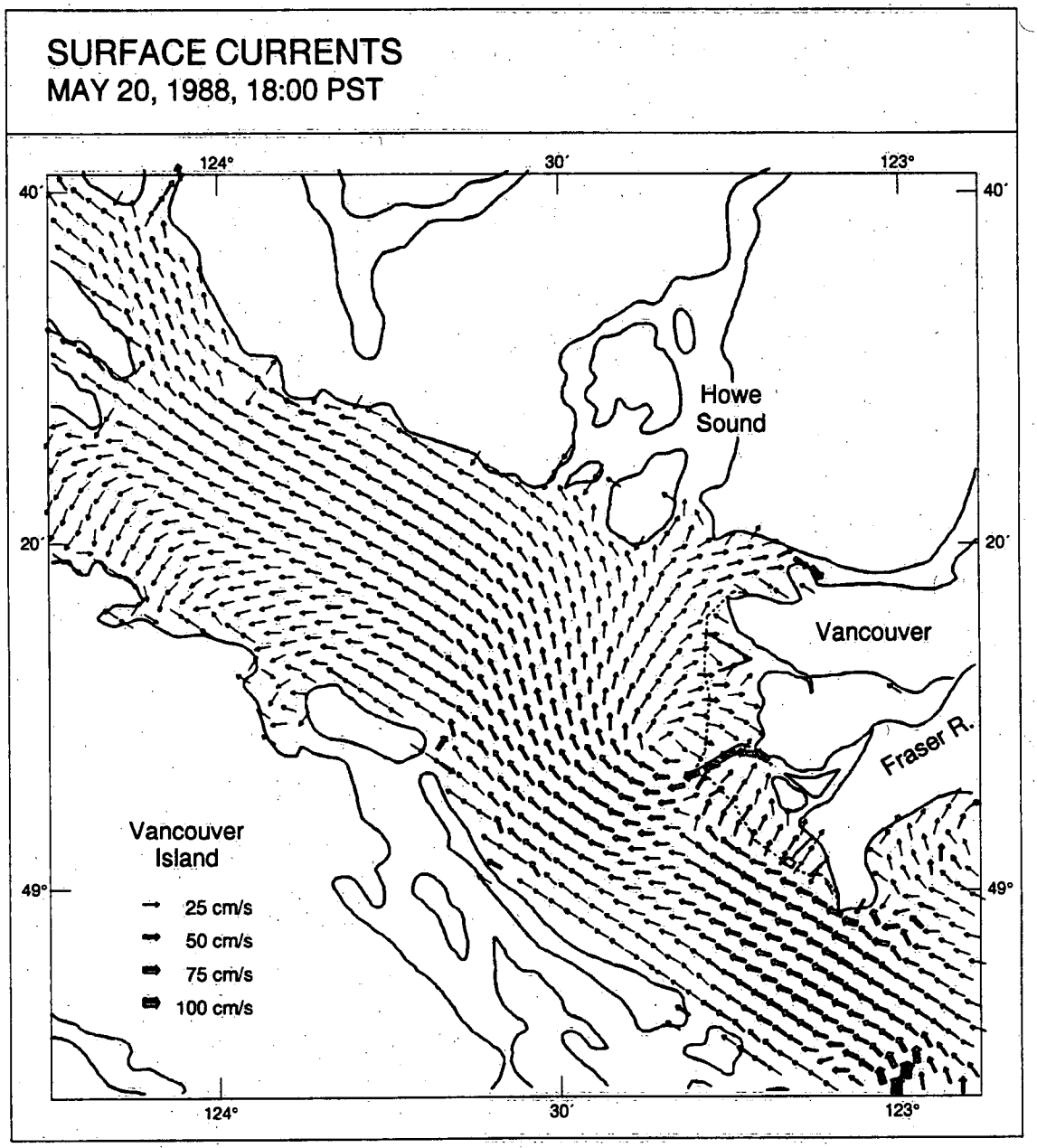

Figure 10: Surface current field predicted by GF4 for 18:00 PST on May 20, 1988, corresponding to a flooding tide.

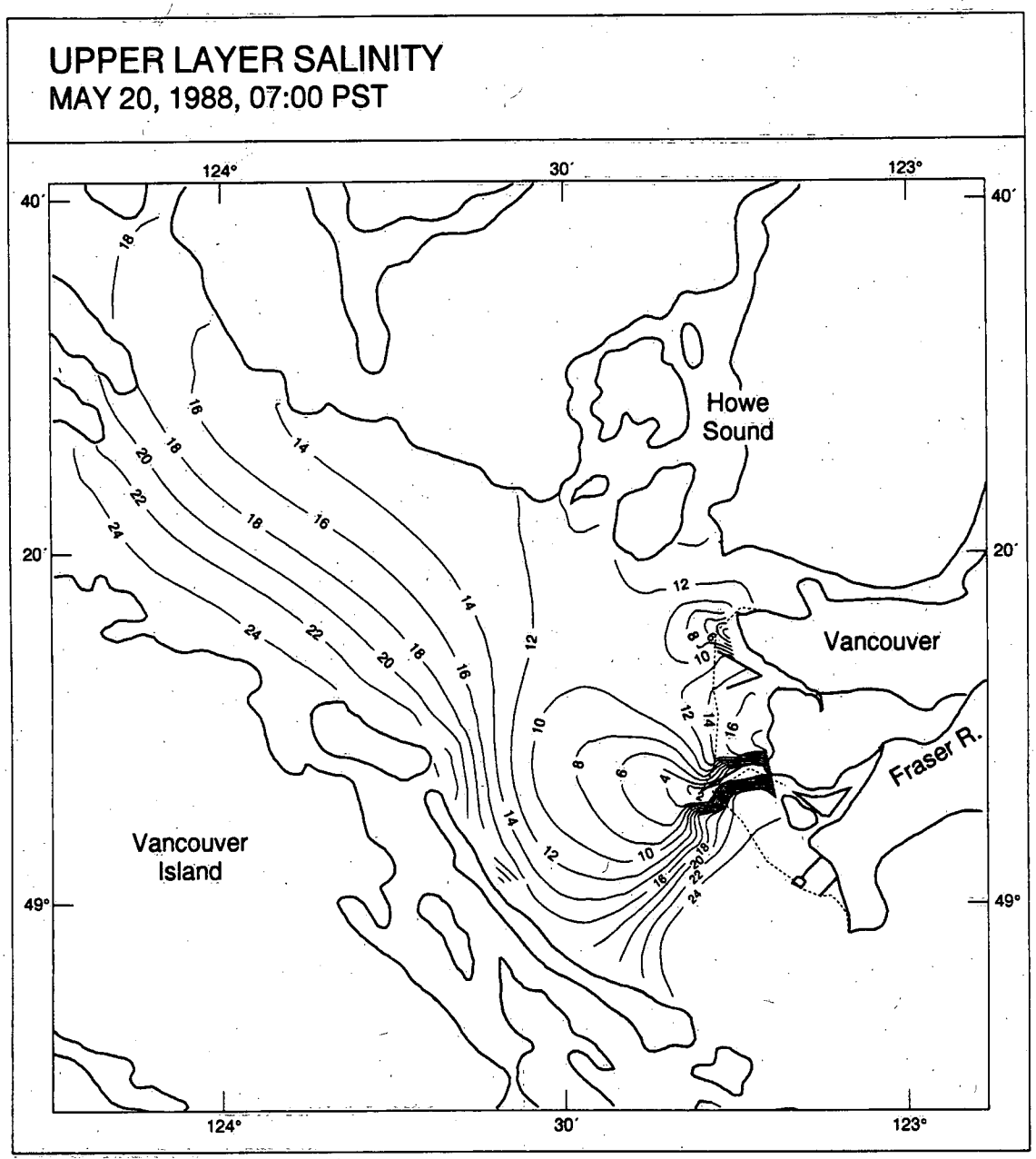

Figure 11: Upper layer salinity field predicted by GF4 for 07:00 PST on May 20, 1988, corresponding to high water.

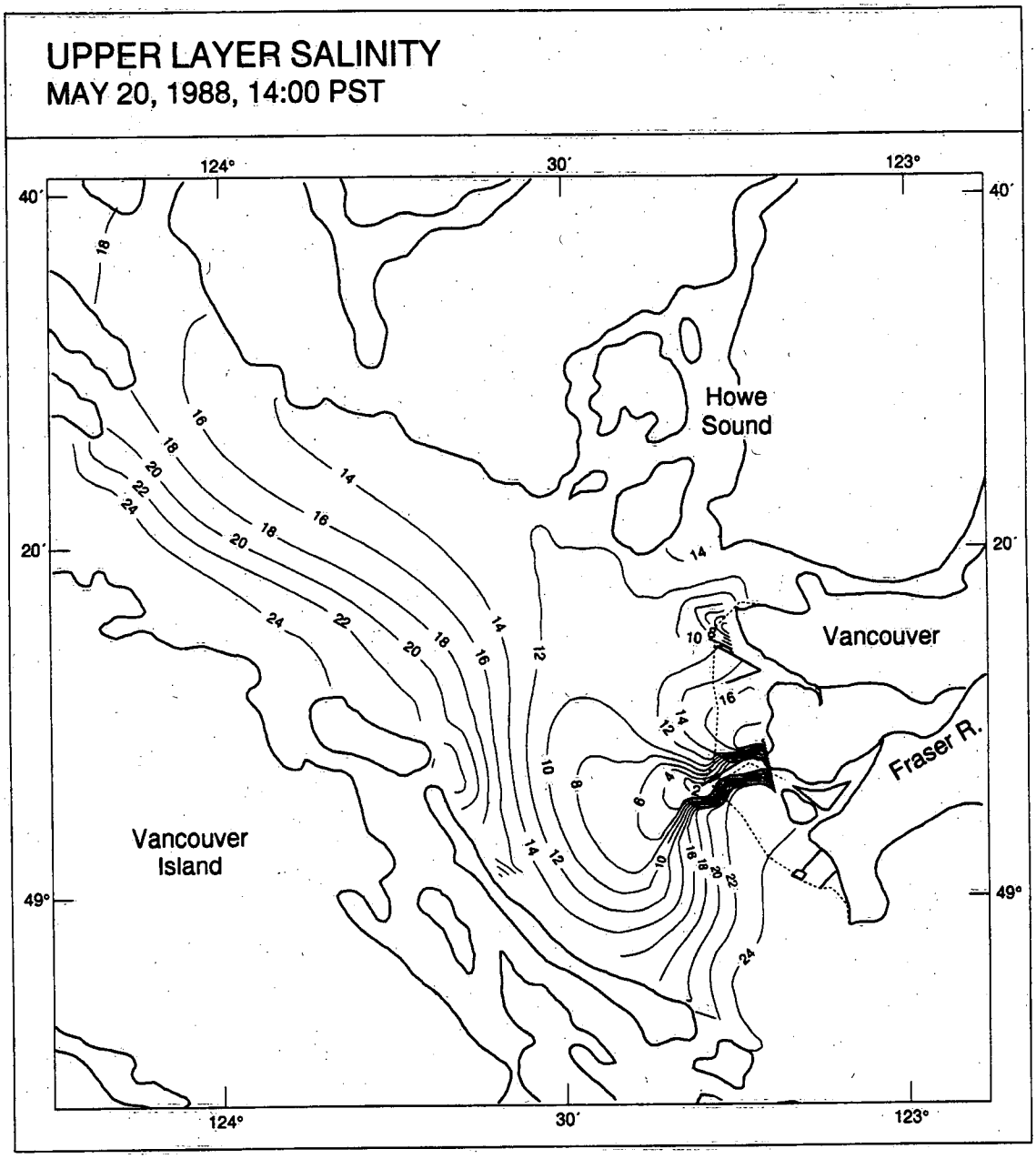

Figure 12: Upper layer salinity field predicted by GF4 for 14:00 PST on May 20, 1988, corresponding to high water.

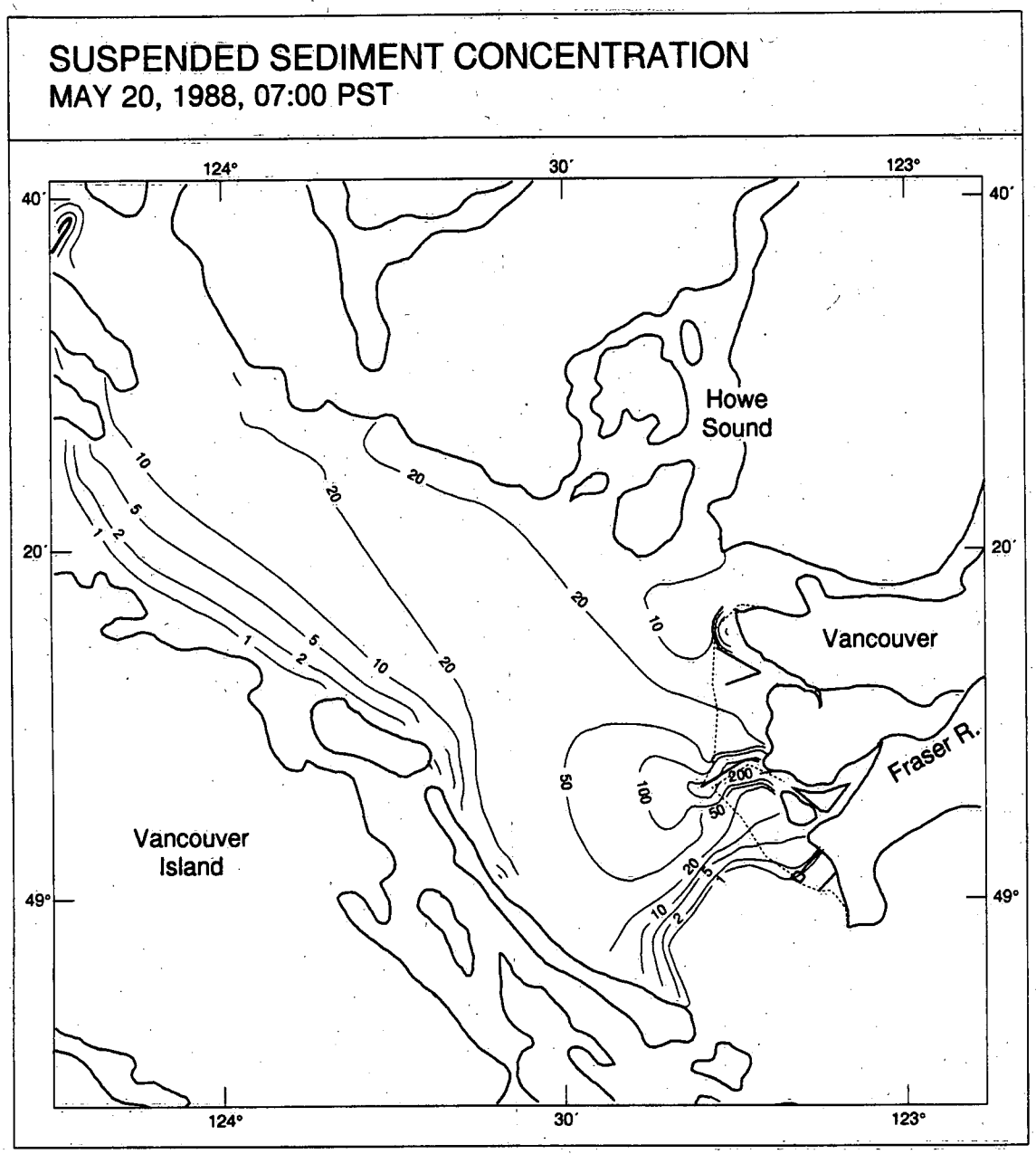

Figure 13: Upper layer suspended sediment concentration field predicted by GF4 for 07:00 PST on May 20, 1988, corresponding to high water. Units of concentration are mg L^{-1}. The solid squares indicate stations that are 4.5 and 9 km from the river mouth for which time series are plotted in Figure 15.

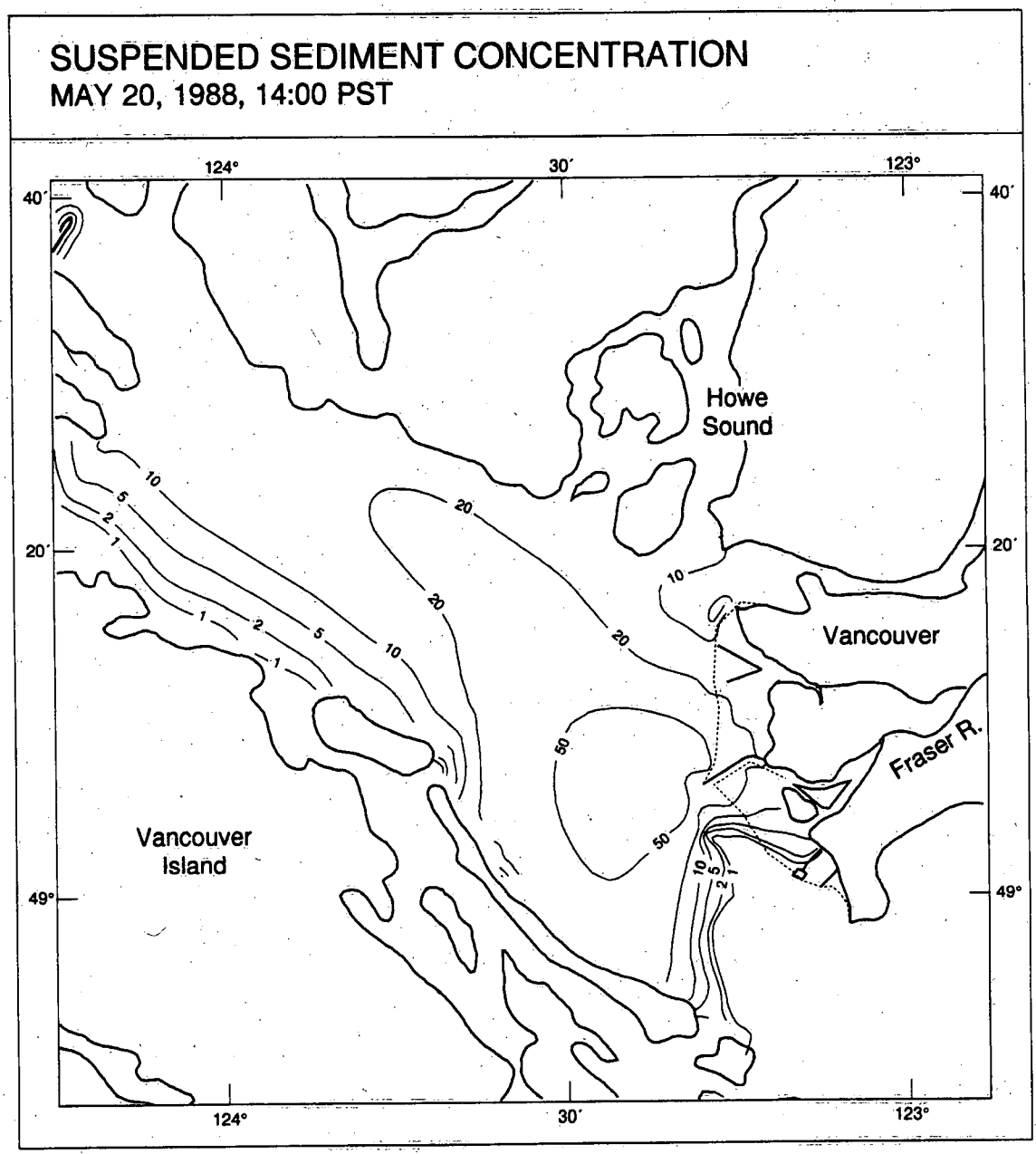

Figure 14: Upper layer suspended sediment concentration field predicted by GF4 for 20:00 PST on May 20, 1988, corresponding to high water. Units of concentration are mg L^{-1}.

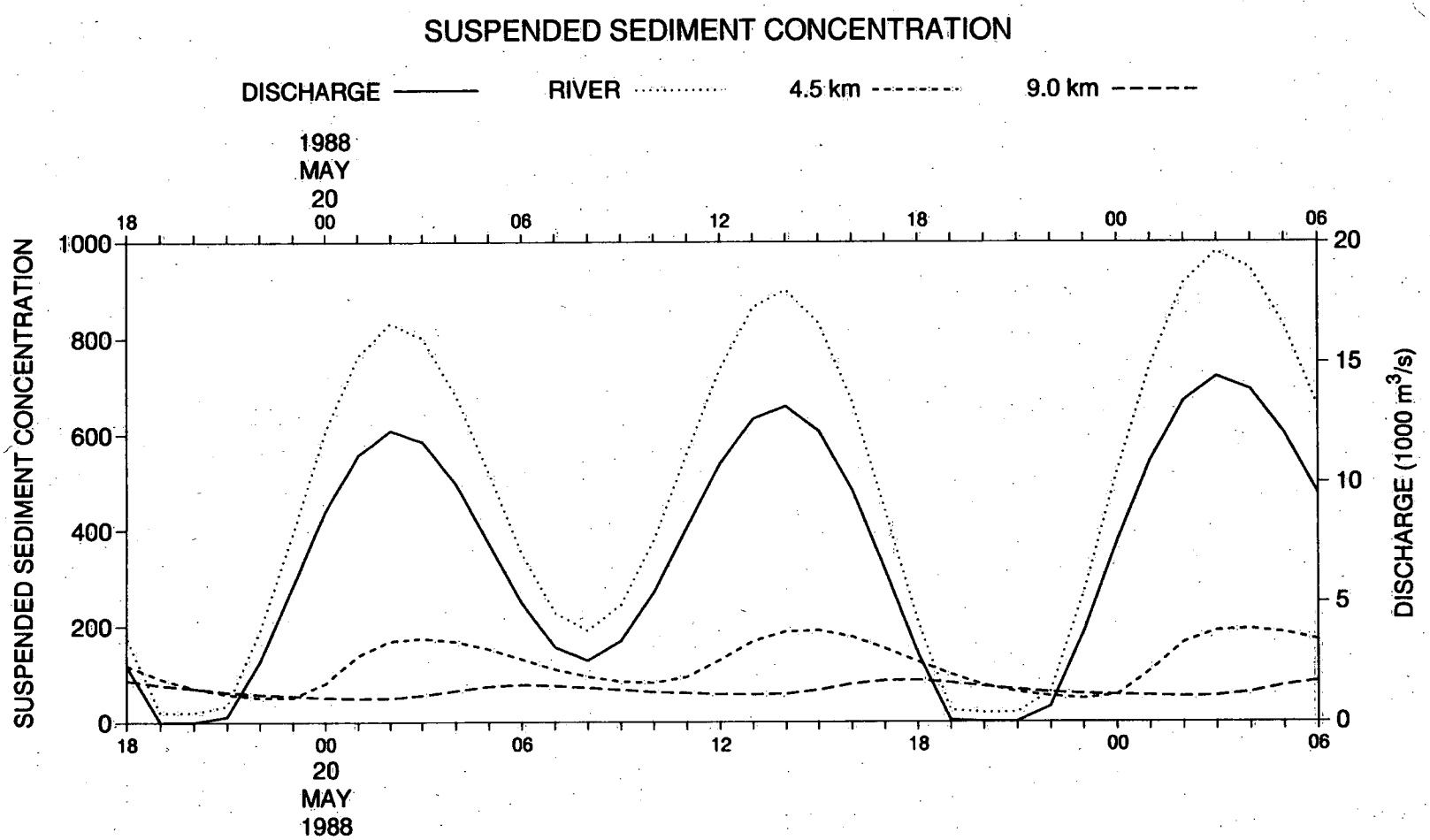

Figure 15: Time-series of suspended sediment concentrations at the river mouth and at 4.5 and 9.0 km downstream from the river mouth over the period from 18:00 PST on May 19, 1988 to 06:00 PST on May 21, 1988, as predicted by GF4.

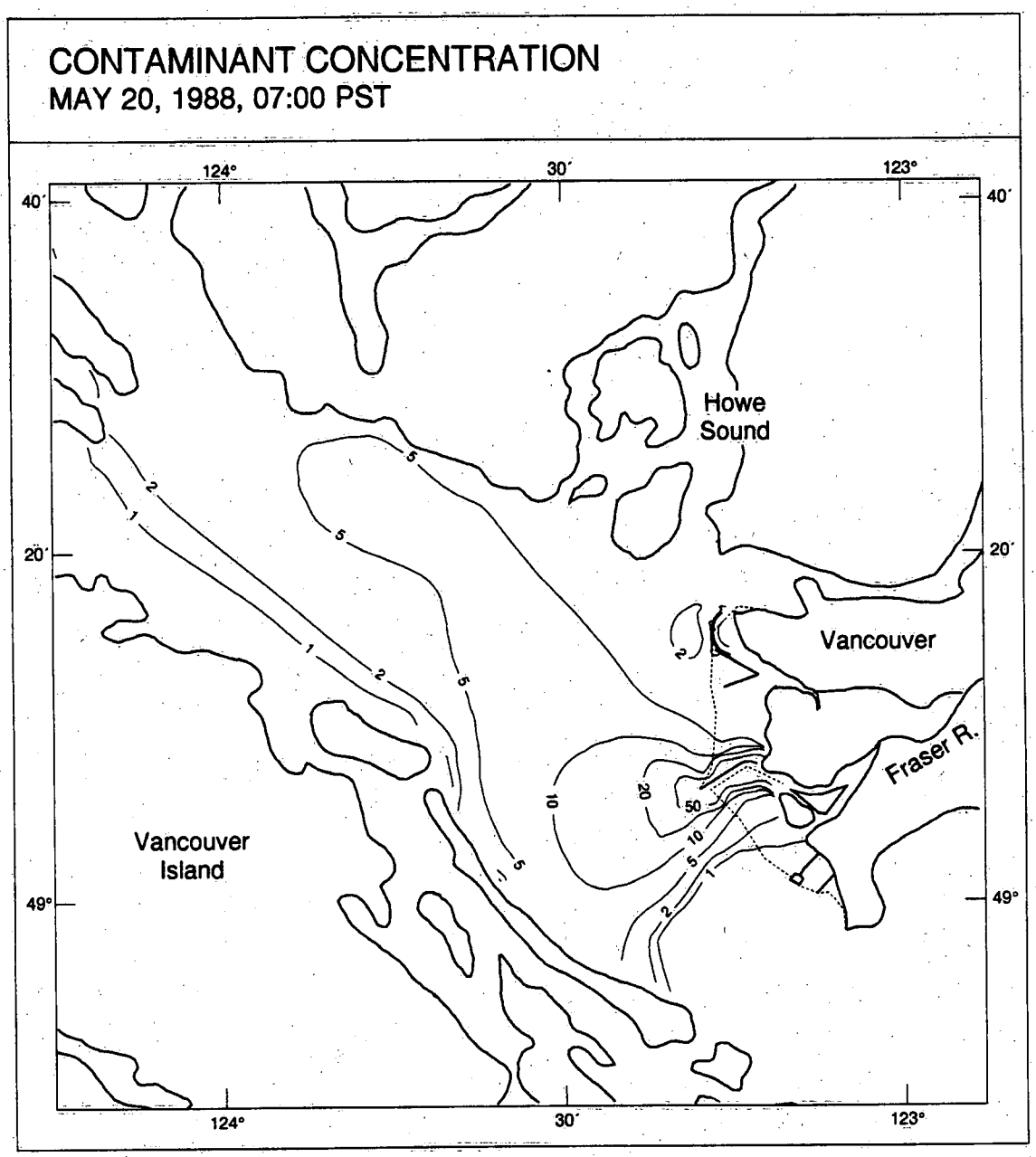

Figure 16: Upper layer contaminant concentration field predicted by GF4 for 07:00 PST on May 20, 1988, corresponding to high water. Adsorption of contaminant onto sediment is incorporated into the calculation. Units of concentration are % of river mouth value. The solid squares indicate stations that are 1.4, 4.5 and 9 km from the river mouth for which time series are plotted in Figure 18.

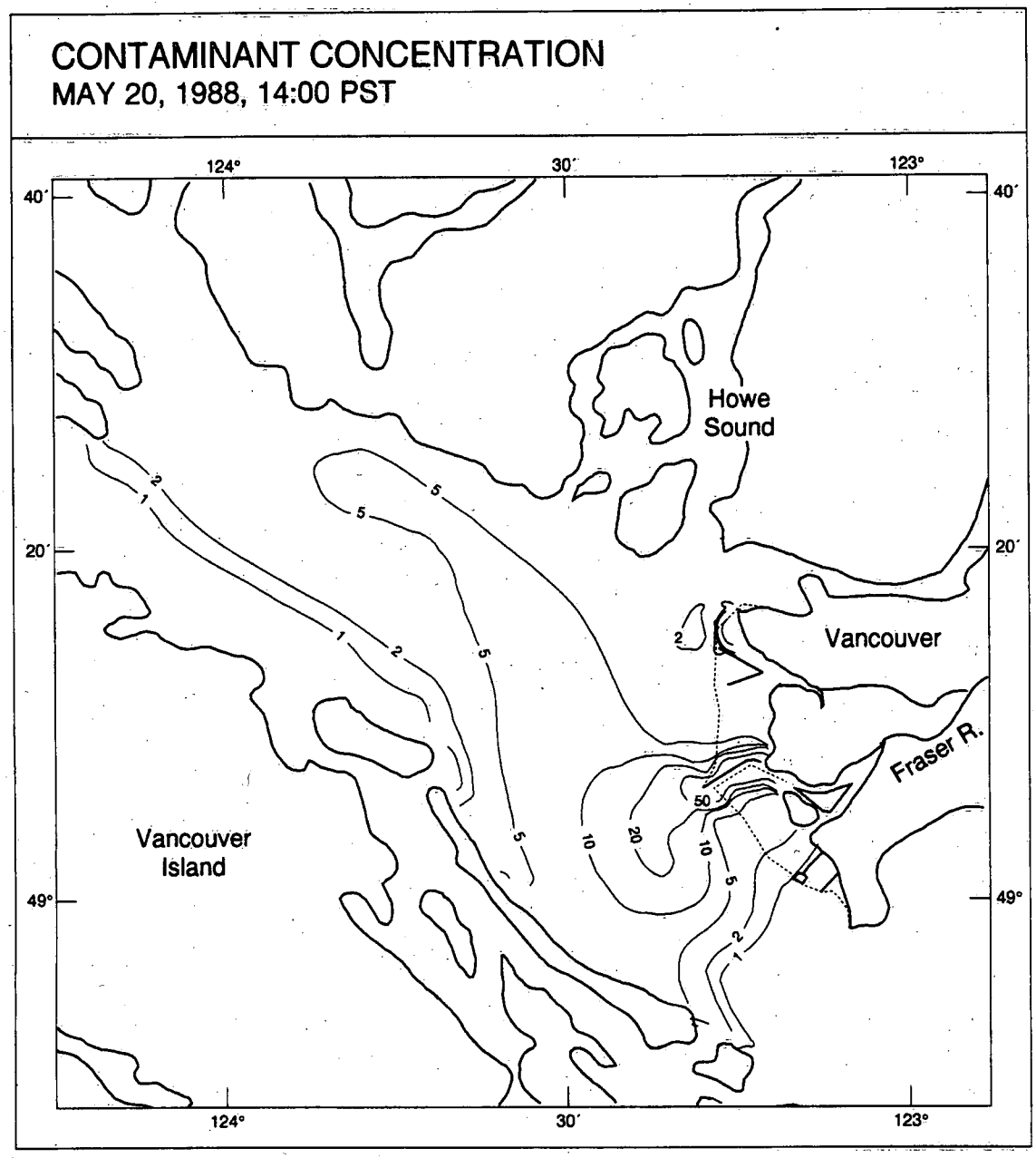

Figure 17: Upper layer contaminant concentration field predicted by GF4 for 14:00 PST on May 20, 1988, corresponding to low water. Adsorption of contaminant onto sediment is incorporated into the calculation. Units of concentration are % of river mouth value.

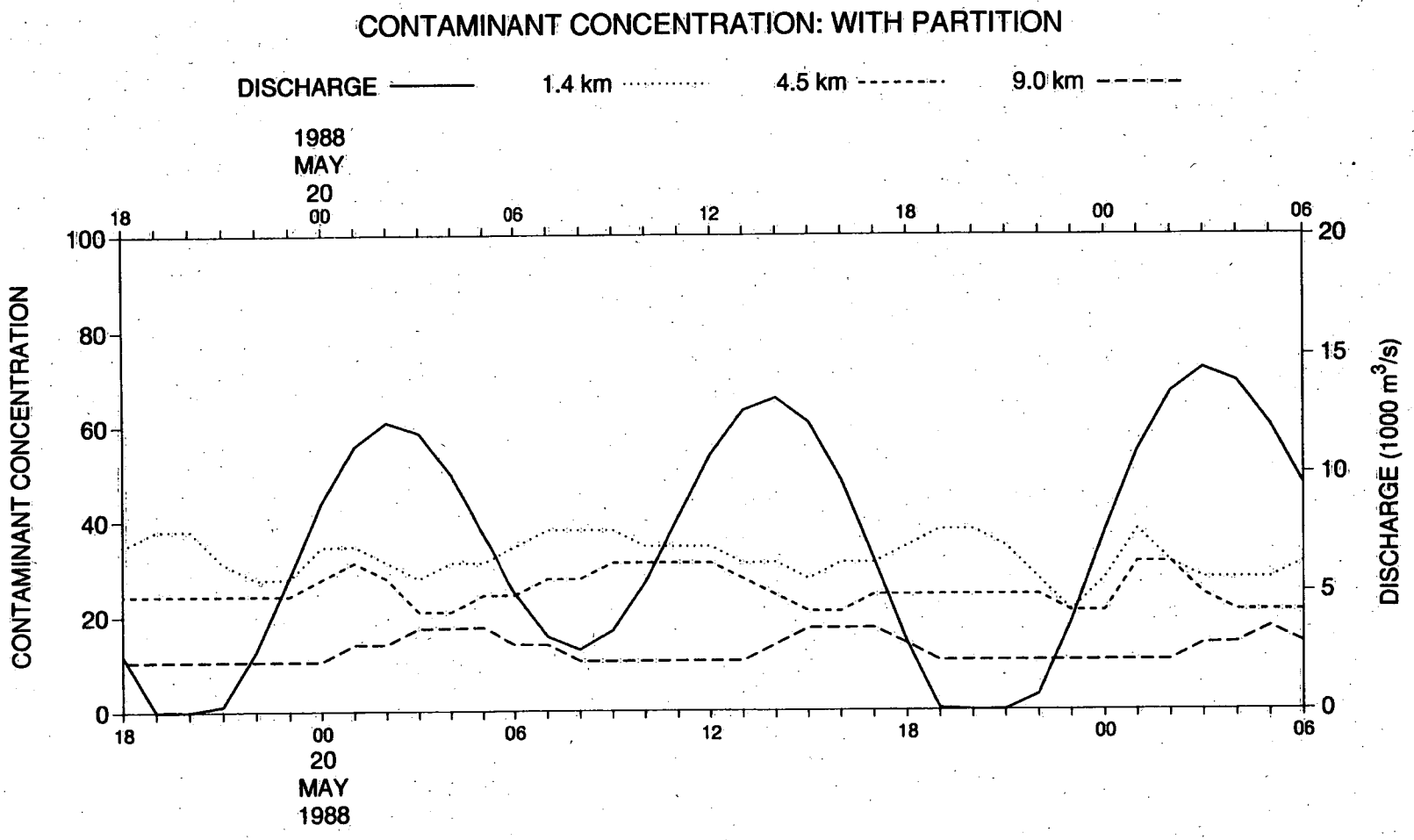

Figure 18: Time-series of contaminant concentrations at distances of 1.4, 4.5 and 9.0 km downstream from the river mouth over the period from 18:00 PST on May 19, 1988 to 06:00 PST on May 21, 1988, as predicted by GF4. Adsorption of contaminant onto the sediment is incorporated in the calculations.

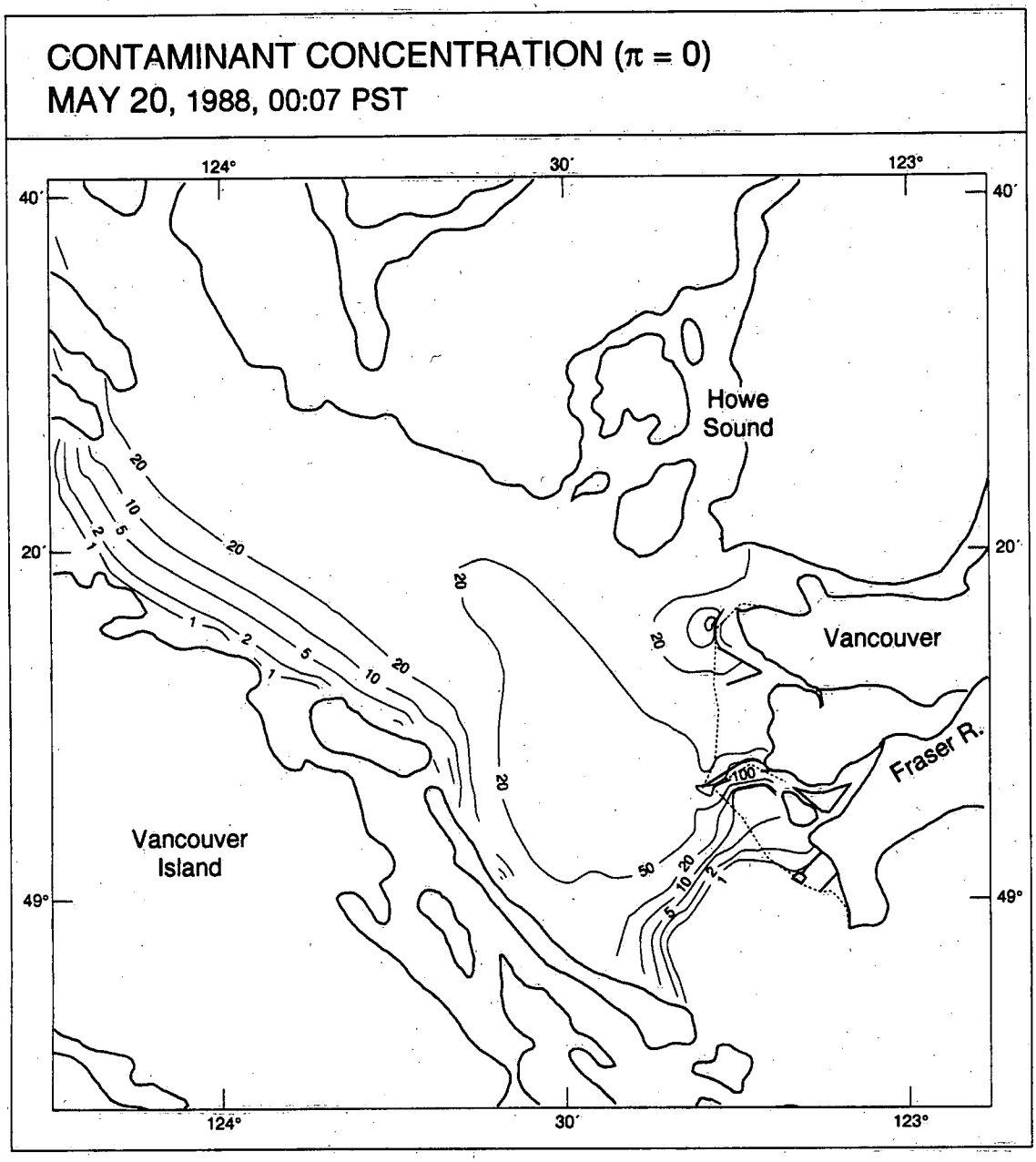

Figure 19: Upper layer contaminant concentration field predicted by GF4 for 07:00 PST on May 20, 1988, corresponding to high water. Adsorption of contaminant onto sediment is not incorporated into the calculation. Units of concentration are % of river mouth value. The solid squares indicate stations that are 1.4, 4.5 and 9 km from the river mouth for which time series are plotted in Figure 21.

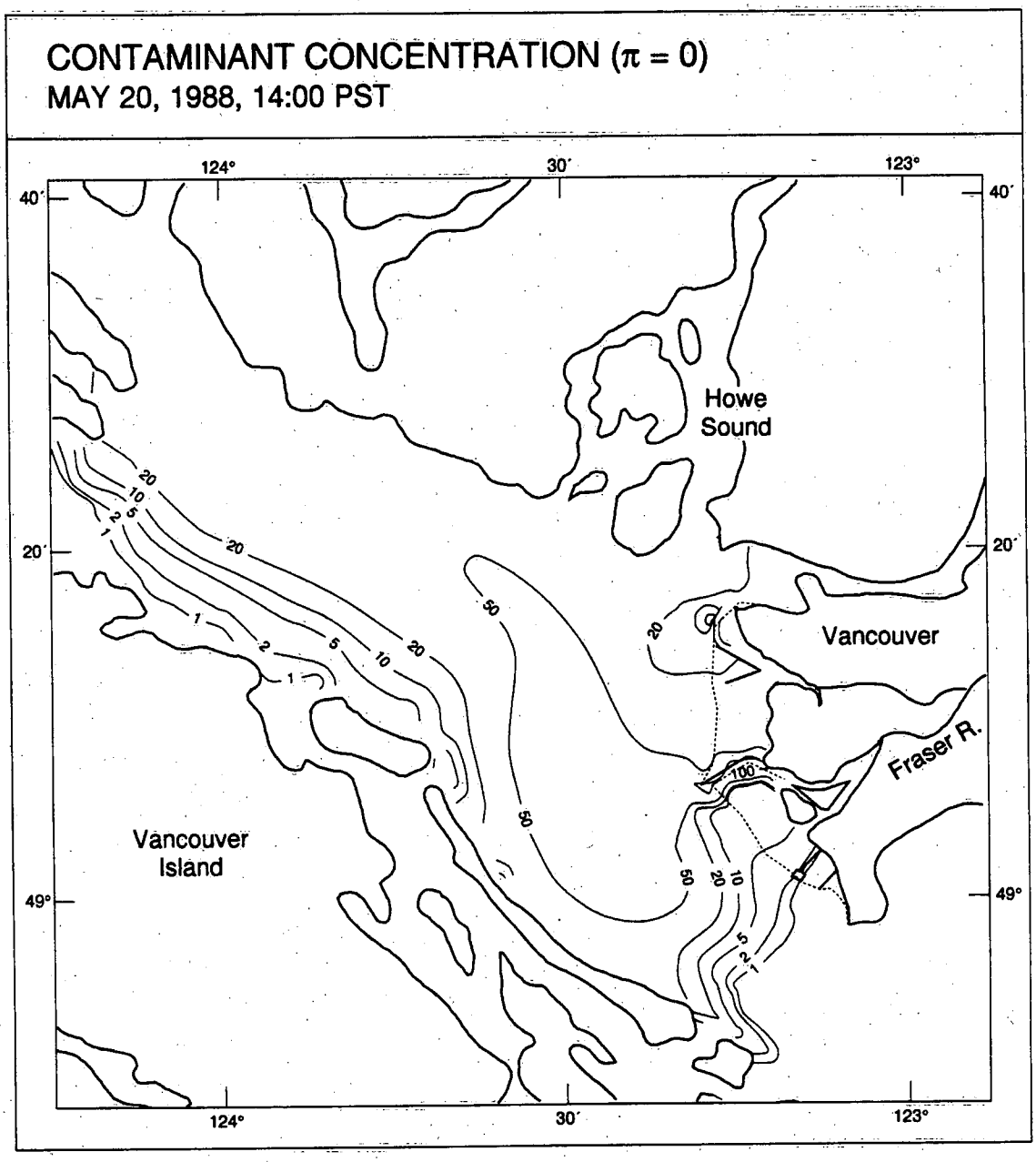

Figure 20: Upper layer contaminant concentration field predicted by GF4 for 14:00 PST on May 20, 1988, corresponding to low water. Adsorption of contaminant onto sediment is not incorporated into the calculation. Units of concentration are % of river mouth value.

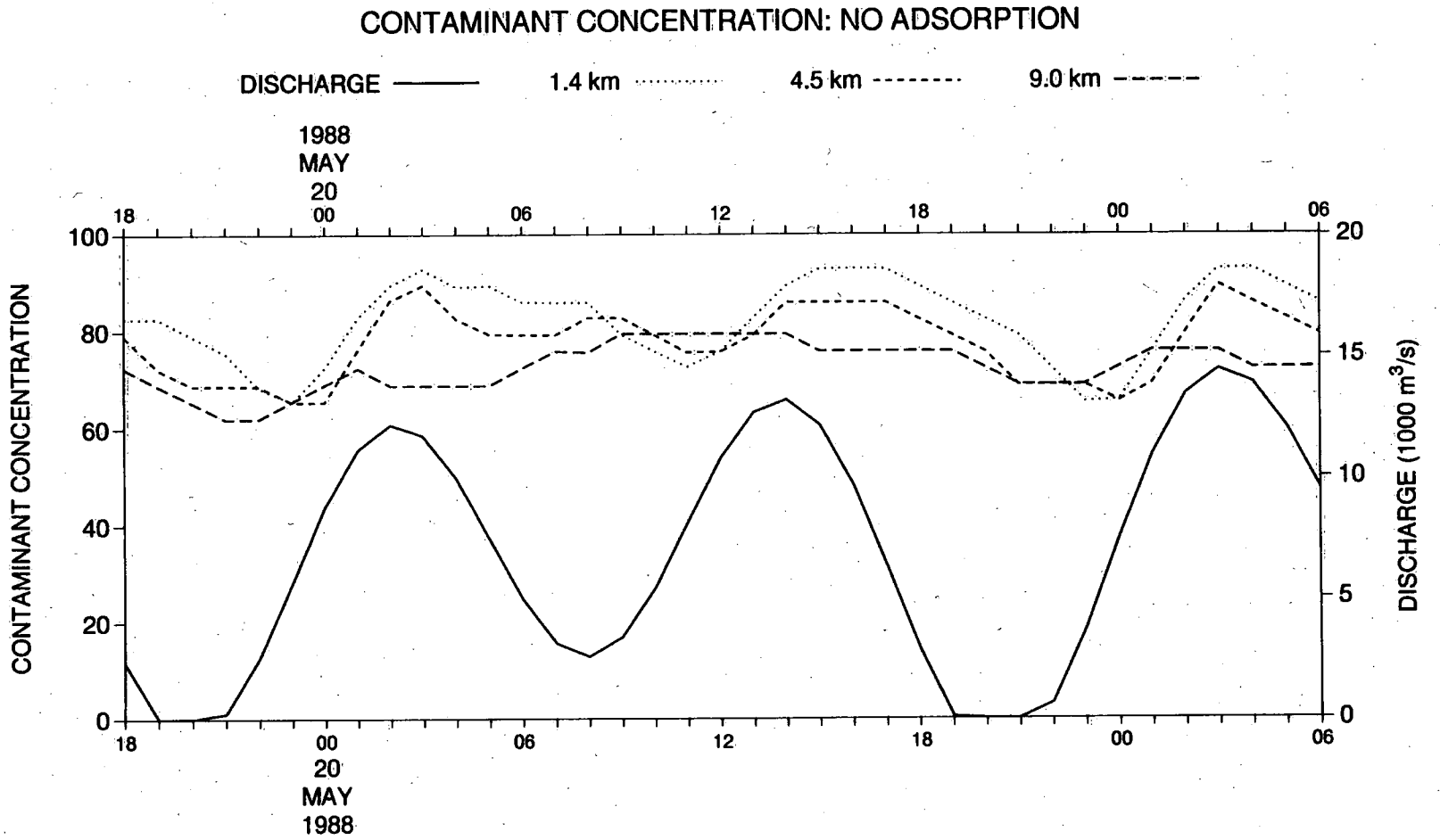

Figure 21: Time-series of contaminant concentrations at distances of 1.4, 4.5 and 9.0 km downstream from the river mouth over the period from 18:00 PST on May 19, 1988 to 06:00 PST on May 21, 1988, as predicted by GF4. Adsorption of contaminant onto the sediment is not incorporated in the calculations.

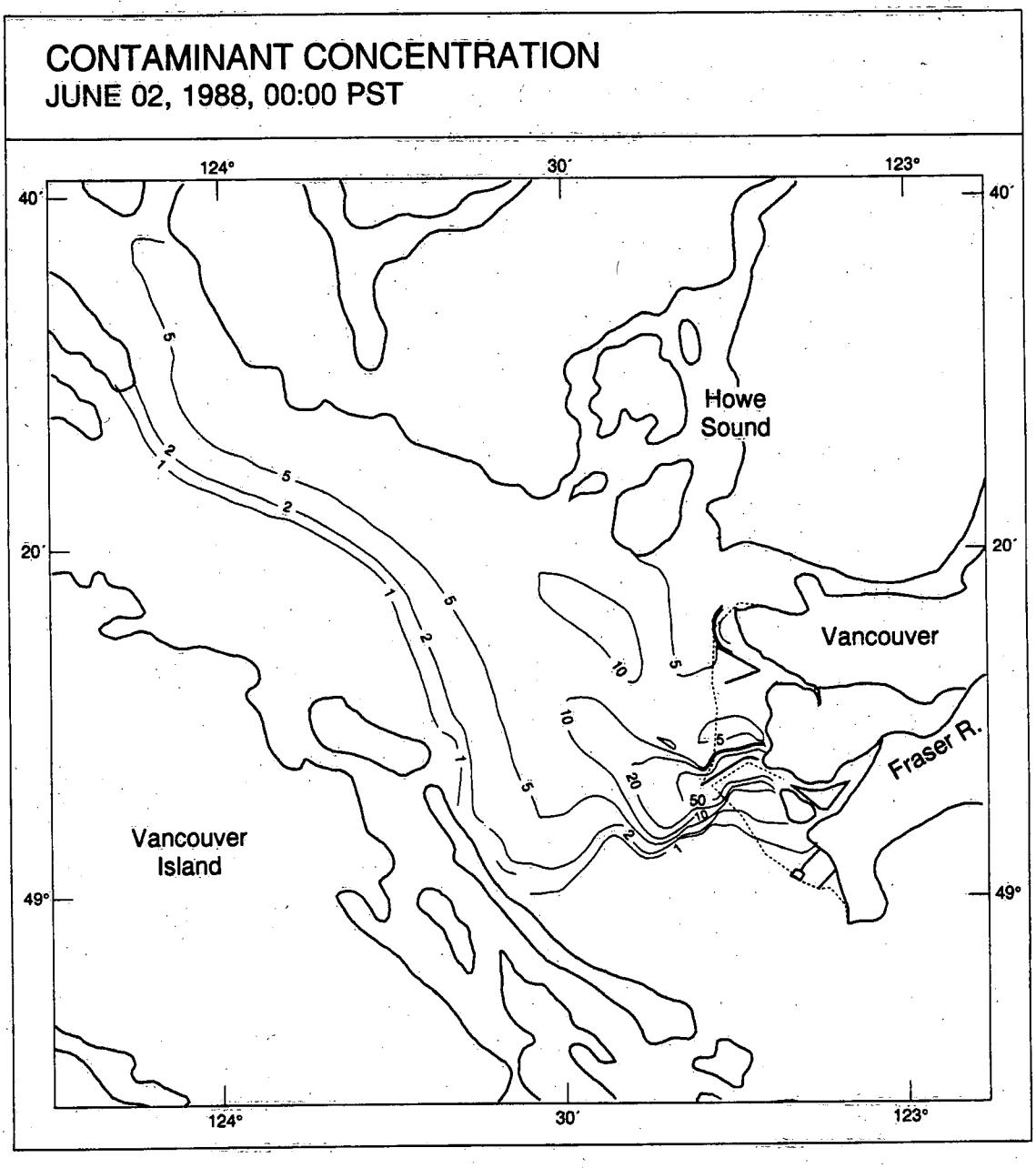

Figure 22: Upper layer contaminant concentration field predicted by GF4 for 00:00 PST on June 2, 1988. Adsorption of contaminant onto sediment is incorporated into the calculation. Southeasterly winds were prevailing at the time. Units of concentration are % of river mouth value.

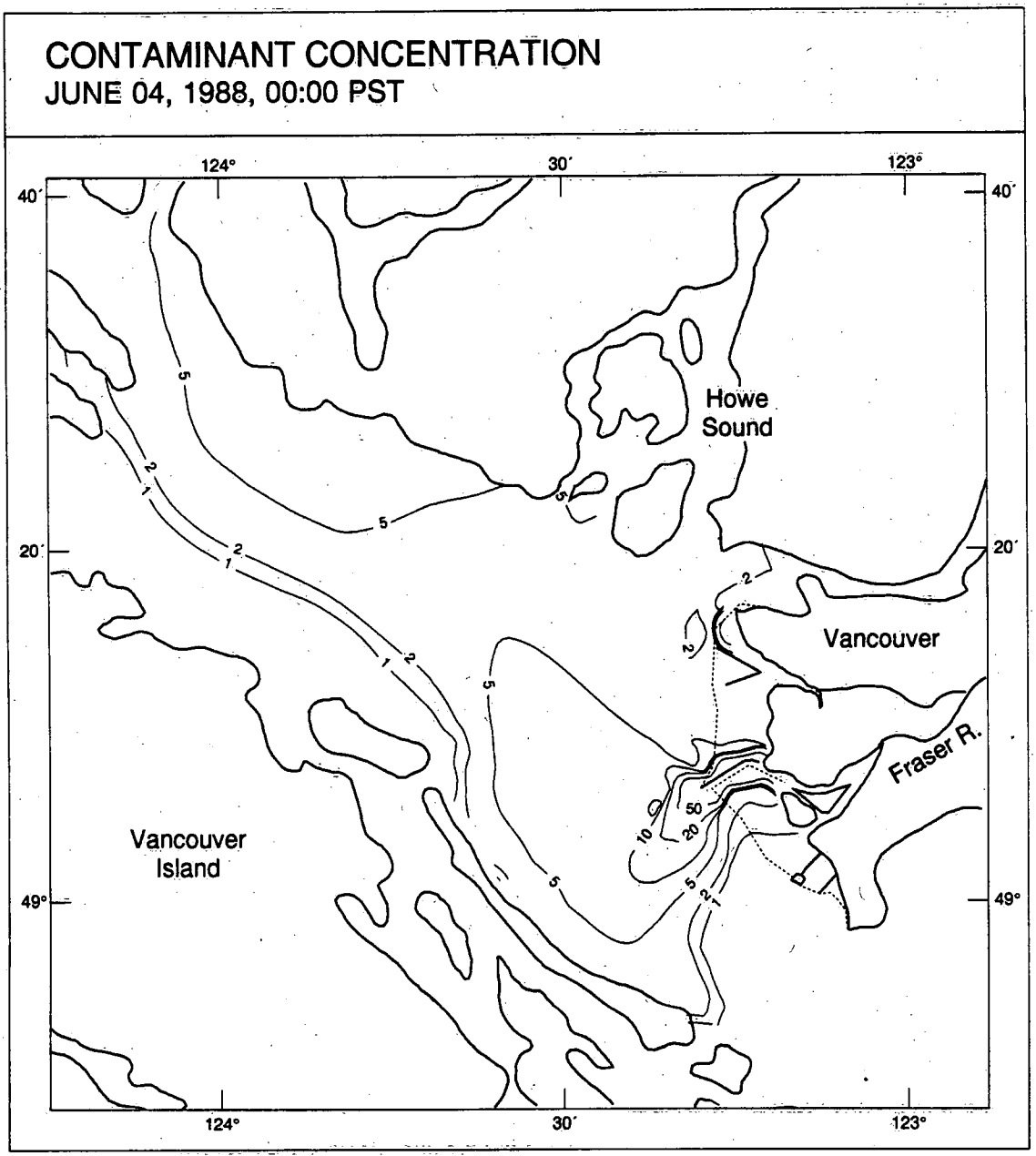

Figure 23: Upper layer contaminant concentration field predicted by GF4 for 00:00 PST on June 4, 1988. Adsorption of contaminant onto sediment is incorporated into the calculation. Northwesterly winds were prevailing at the time. Units of concentration are % of river mouth value.

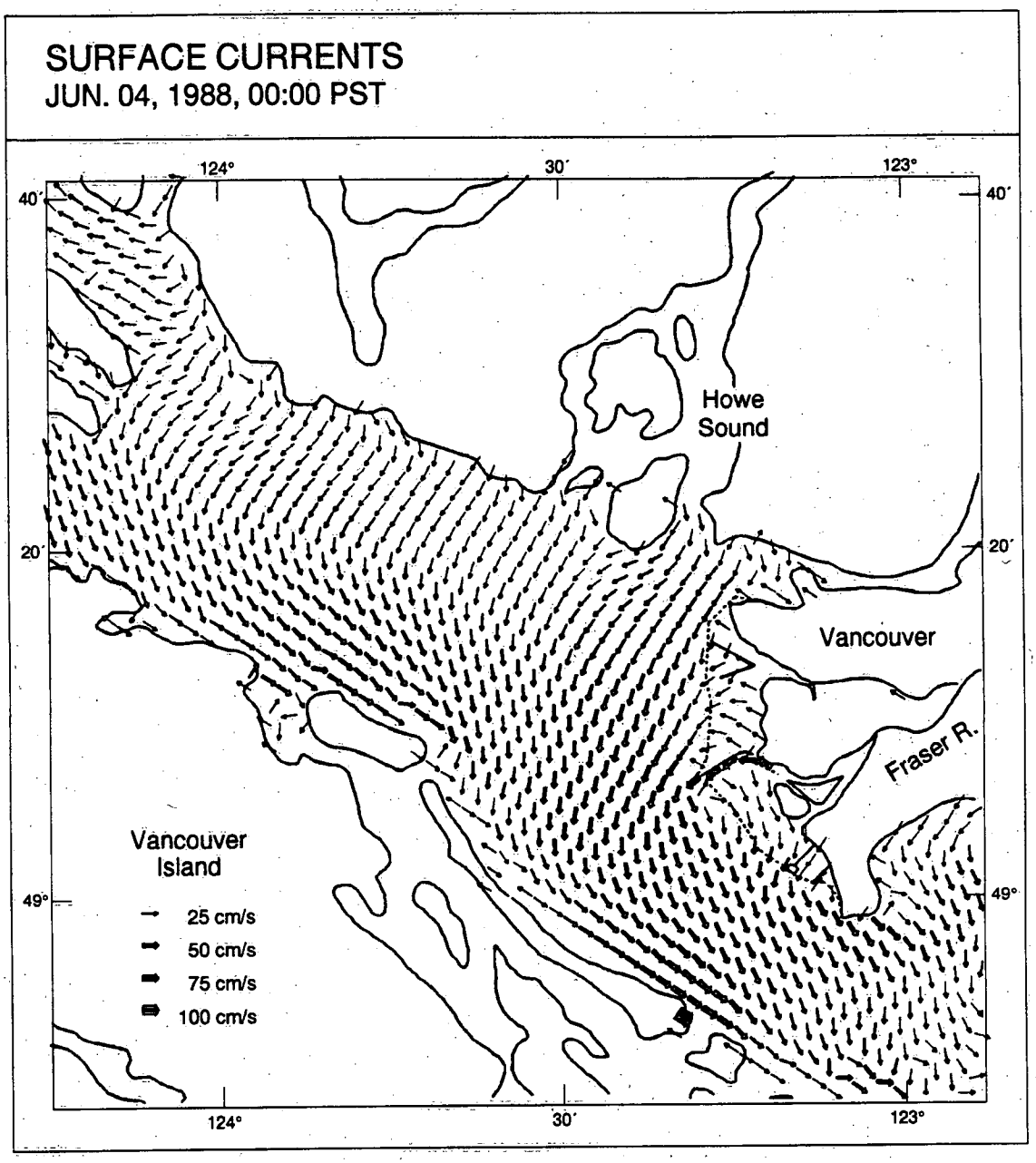

Figure 24: Surface current field predicted by GF4 for 00:00 PSTon June 4, 1988.

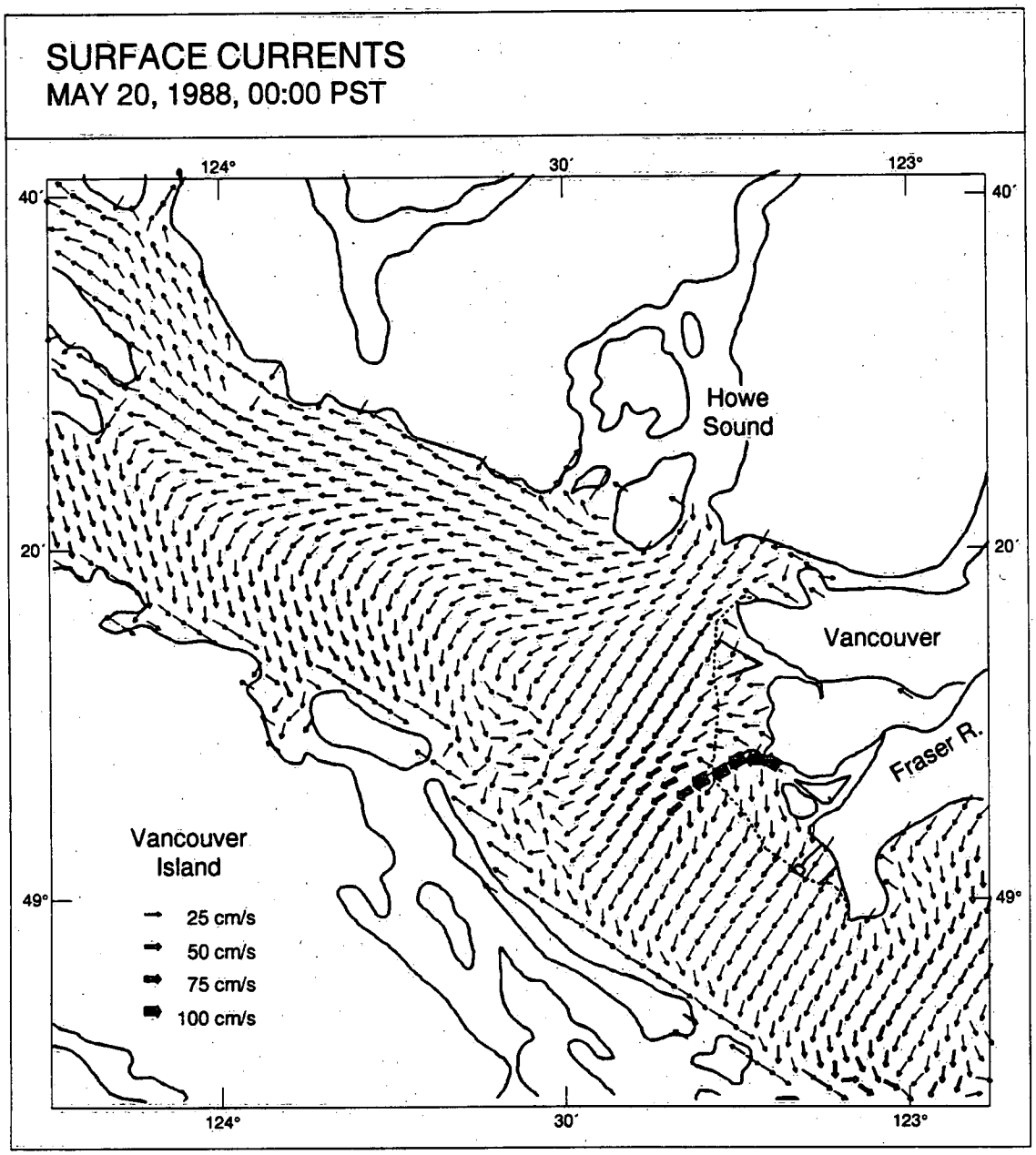

Figure 25: Surface current field predicted by GF4 for 00:00 PST on May 20, 1988.

R7820

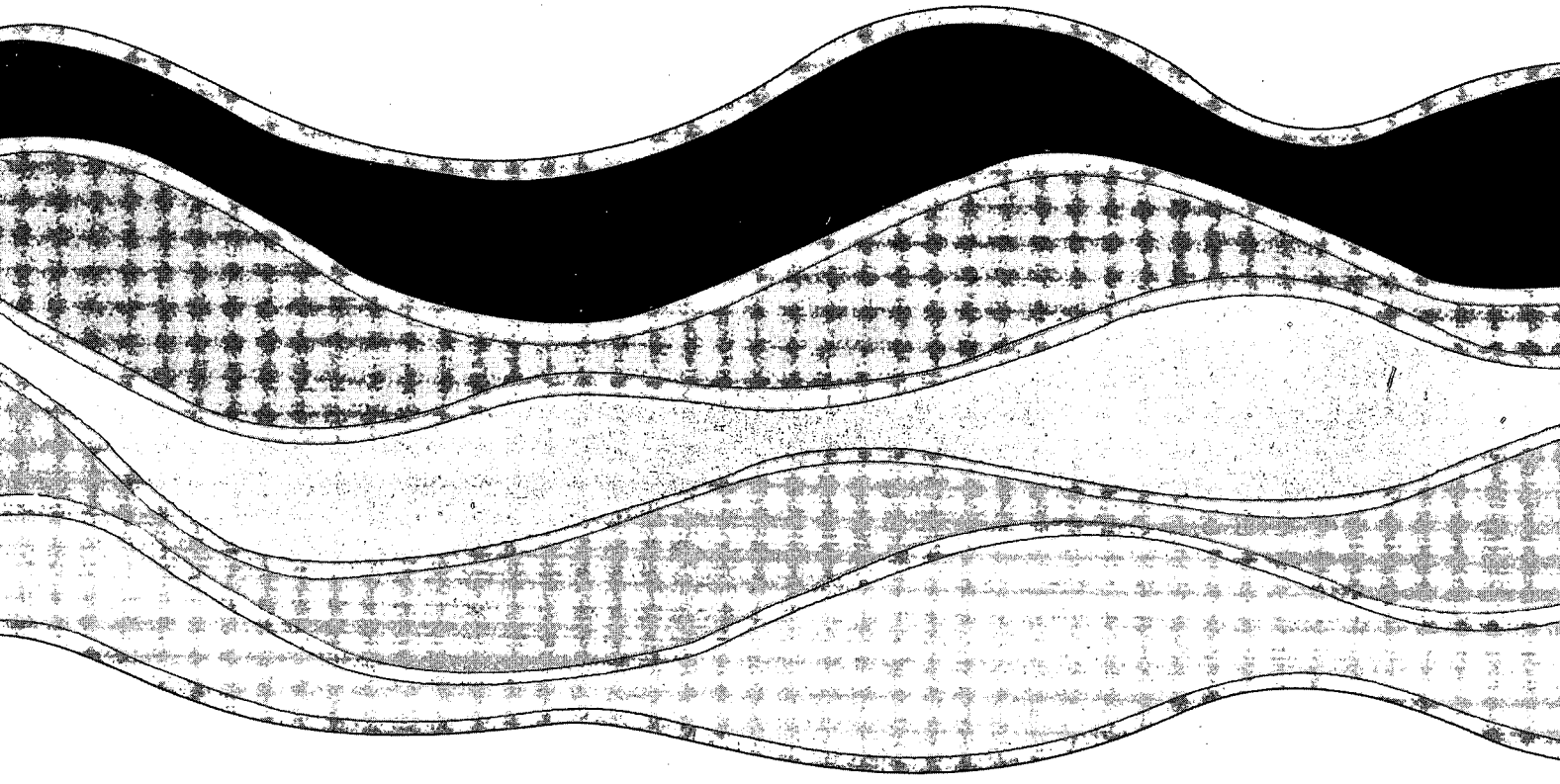

NATIONAL WATER RESEARCH INSTITUTE
P.O. BOX 5050, BURLINGTON, ONTARIO L7R 4A6

Environment Canada Environnement Canada

Canada

INSTITUT NATIONAL DE RECHERCHE SUR LES EAUX
C.P. 5050, BURLINGTON (ONTARIO) L7R 4A6